Supporting Information

Trimethoxybenzene- and trimethylbenzene-based compounds bearing imidazole, indole and pyrrole groups as recognition units: Synthesis and evaluation of the binding properties towards carbohydrates

Jan-Ruven Rosien, Wilhelm Seichter and Monika Mazik*

Institut für Organische Chemie, Technische Universität Bergakademie Freiberg,

Leipziger Straße 29, 09596 Freiberg, Germany

monika.mazik@chemie.tu-freiberg.de

1 Plots of the chemical shifts of the receptor resonances as a function of added carbohydrate (EQNMR program).

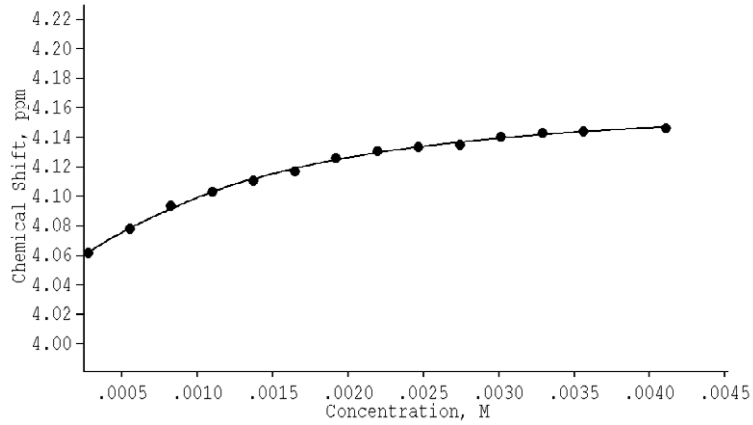

Figure S1. Plot of the observed chemical shifts of the CH_2 resonances of **14a** as a function of added β-glucoside **27a** in $CDCl_3$ (1:1 binding model).

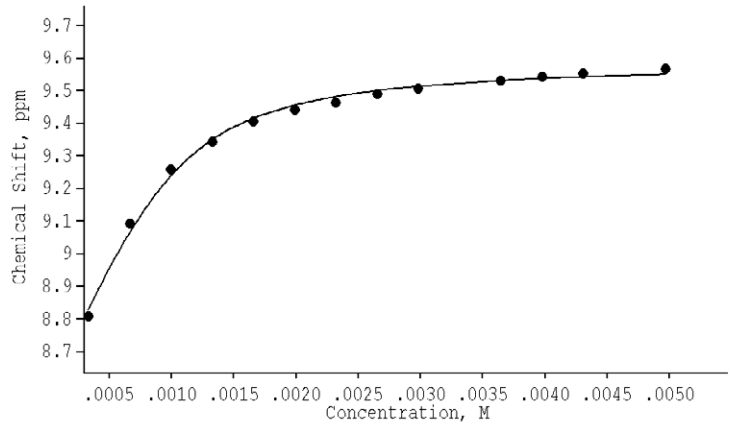

Figure S2. Plot of the observed chemical shifts of the NH-indole resonances of **14b** as a function of added β-glucoside **27a** in $CDCl_3$ (1:1 binding model).

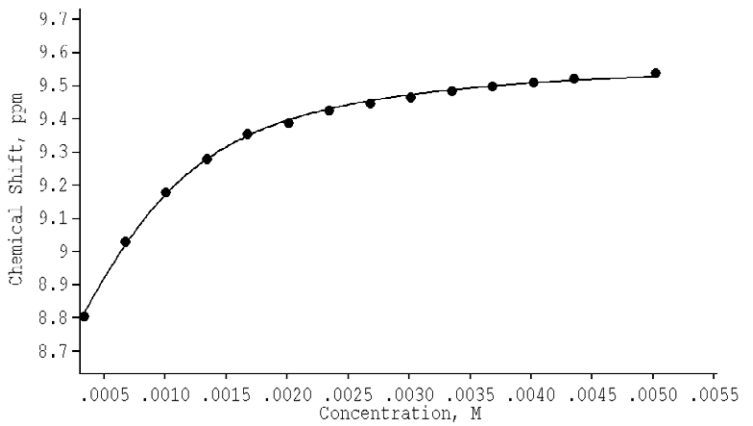

Figure S3. Plot of the observed chemical shifts of the NH-pyrrole resonances of **16a** as a function of added β-glucoside **27a** in $CDCl_3$ (1:1 binding model).

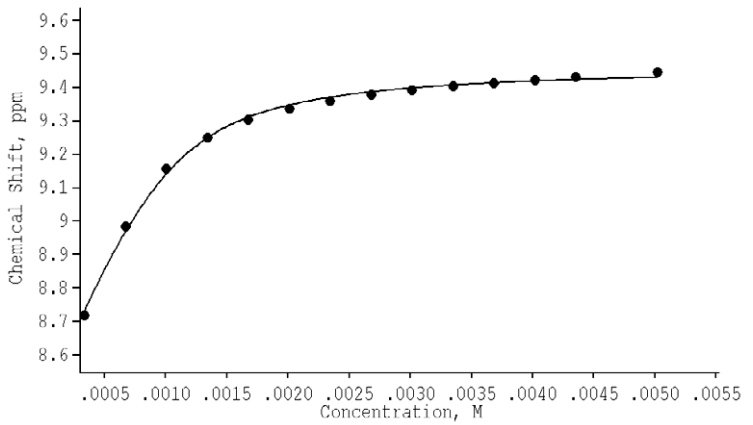

Figure S4. Plot of the observed chemical shifts of the NH-pyrrole resonances of **16b** as a function of added β-glucoside **27a** in $CDCl_3$ (1:1 binding model).

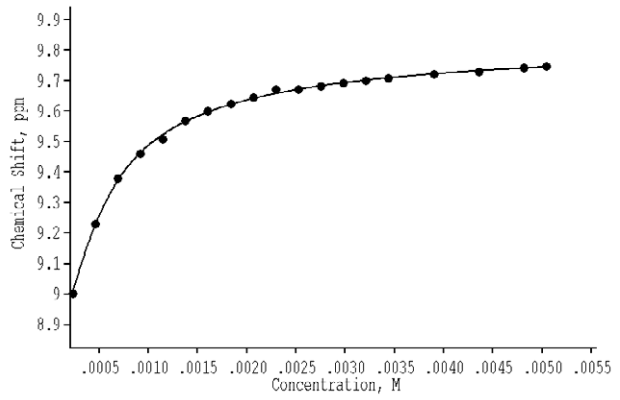

Figure S5. Plot of the observed chemical shifts of the NH-indole resonances of **14a** as a function of added β-galactoside **29a** in $CDCl_3$ ("mixed" 1:1 and 2:1 receptor-sugar binding model).

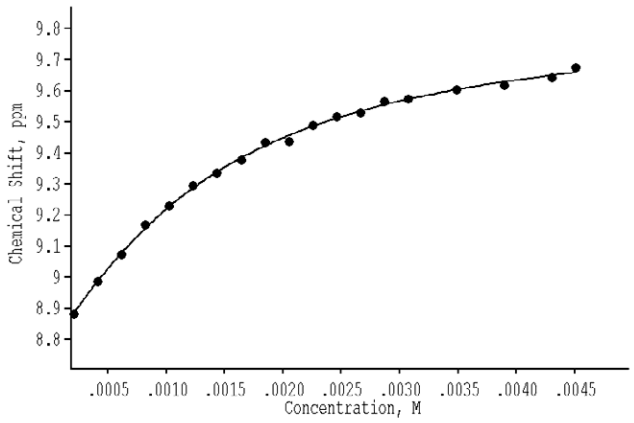

Figure S6. Plot of the observed chemical shifts of the NH-indole resonances of **14a** as a function of added α-galactoside **30a** in $CDCl_3$ (1:1 binding model).

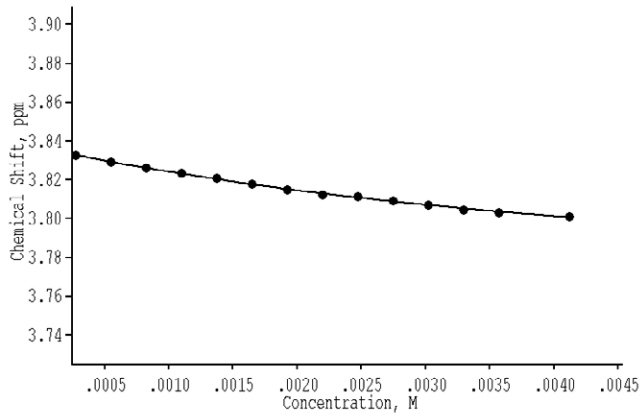

Figure S7. Plot of the observed chemical shifts of the CH_2 resonances of **15a** as a function of added β-glucoside **27a** in $CDCl_3$ (1:1 binding model).

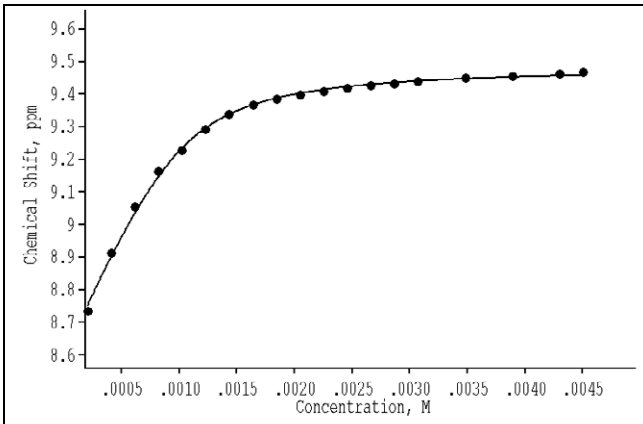

Figure S8. Plot of the observed chemical shifts of the NH-pyrrole resonances of **16a** as a function of added β-galactoside **29a** in $CDCl_3$ (1:1 binding model).

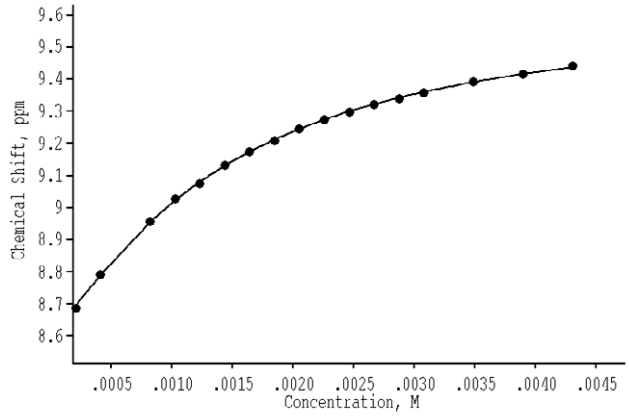

Figure S9. Plot of the observed chemical shifts of the NH-pyrrole resonances of **16a** as a function of added α-galactoside **30a** in $CDCl_3$ (1:1 binding model).

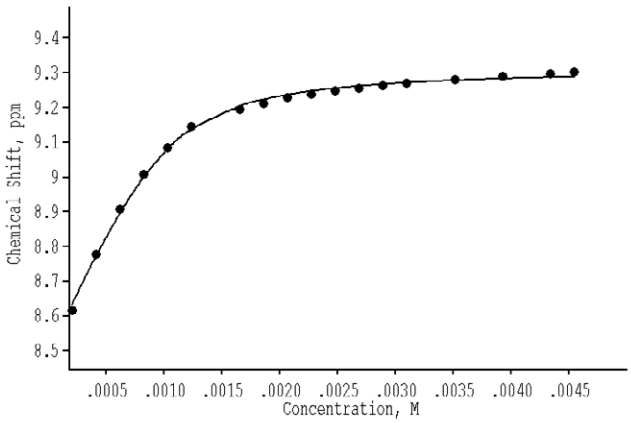

Figure S10. Plot of the observed chemical shifts of the NH-pyrrole resonances of **16b** as a function of added β-galactoside **29a** in $CDCl_3$ (1:1 binding model).

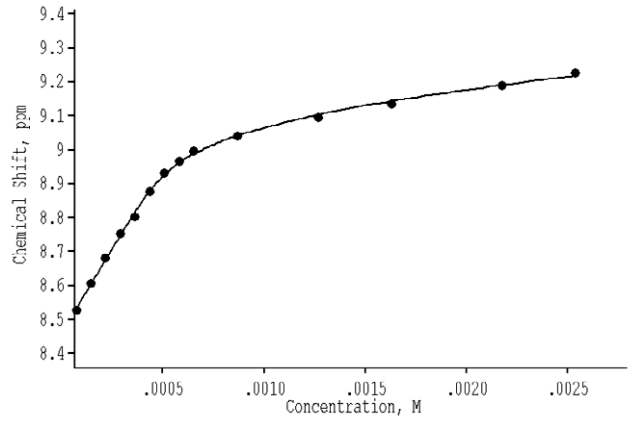

Figure S11. Plot of the observed chemical shifts of the NH-pyrrole resonances of **16b** as a function of added β-maltoside **31** in $CDCl_3$ ("mixed" 1:1 and 2:1 receptor-sugar binding model).

2 Representative mole ratio plots

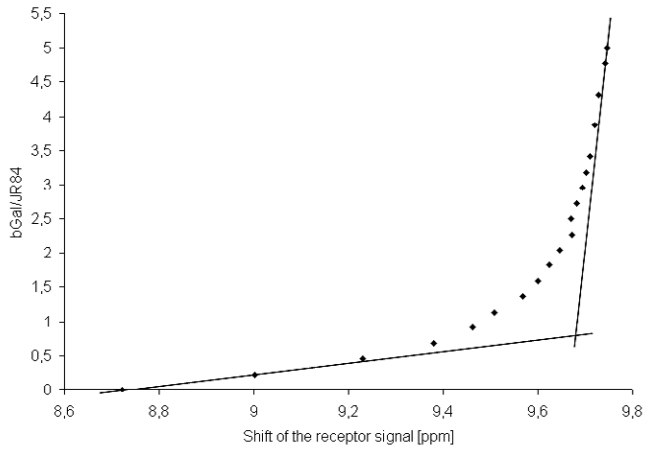

Figure S12. Mole ratio plot: Titration of compound **14a** with β-galactopyranoside **29a** in $CDCl_3$ (analysis of the complexation-induced shift of the NH-indole signal of **14a**).

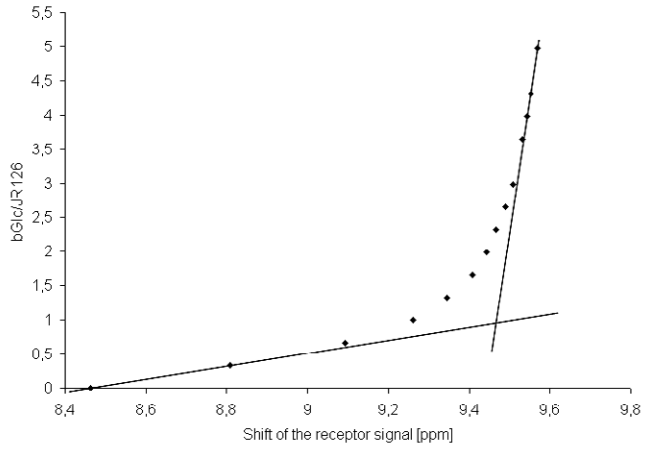

Figure S13. Mole ratio plot: Titration of compound **14b** with β-glucopyranoside **27a** in $CDCl_3$ (analysis of the complexation-induced shift of the NH-indole signal of **14b**).

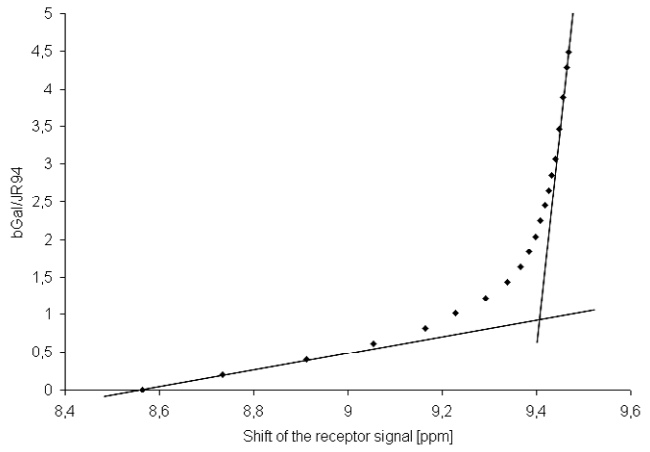

Figure S14. Mole ratio plot: Titration of compound **16a** with β-galactopyranoside **29a** in $CDCl_3$ (analysis of the complexation-induced shift of the NH-pyrrole signal of **16a**).

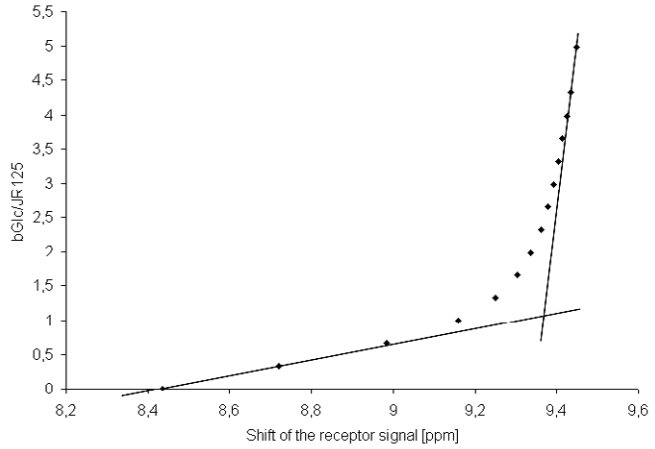

Figure S15. Mole ratio plot: Titration of compound **16b** with β-glucopyranoside **27a** in $CDCl_3$ (analysis of the complexation-induced shift of the NH-pyrrole signal of **16b**).

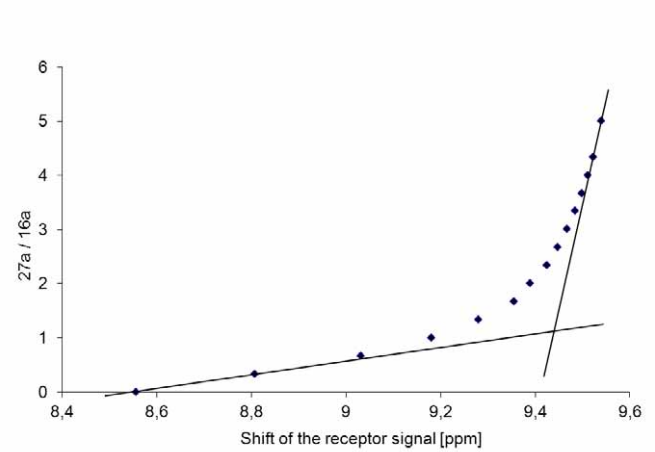

Figure S16. Mole ratio plot: Titration of compound **16a** with β-glucopyranoside **27a** in $CDCl_3$ (analysis of the complexation-induced shift of the NH-pyrrole signal of **16a**).

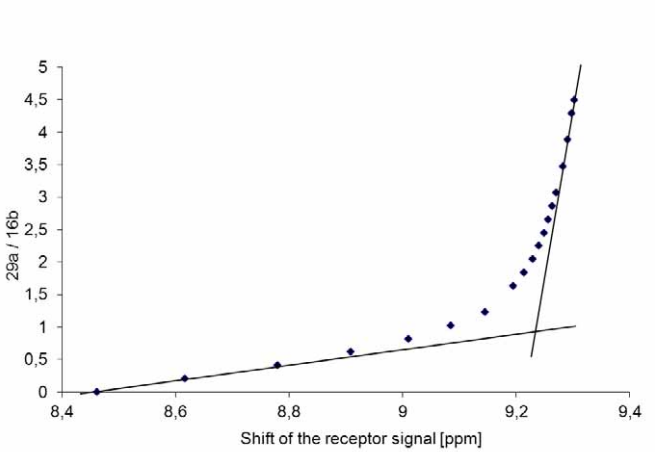

Figure S17. Mole ratio plot: Titration of compound **16b** with β-galactopyranoside **29a** in $CDCl_3$ (analysis of the complexation-induced shift of the NH-pyrrole signal of **16b**).

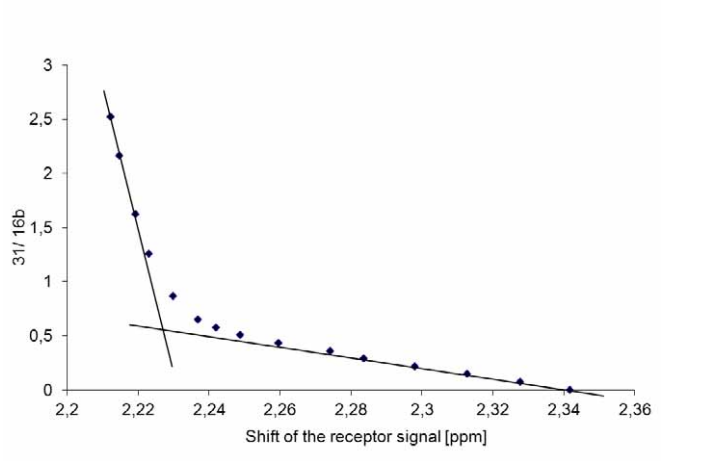

Figure S18. Mole ratio plot: Titration of compound **16b** with β-maltoside **31** in $CDCl_3$ (analysis of the complexation-induced shift of the methoxy signal of **16b**).

3 ^{1}H NMR titrations of compounds **14a**, **14b**, **16a** and **16b** with the tested carbohydrates.

3.1 ^{1}H NMR titrations of compound **14a** with β-glucoside **27a**.

a) b) c)

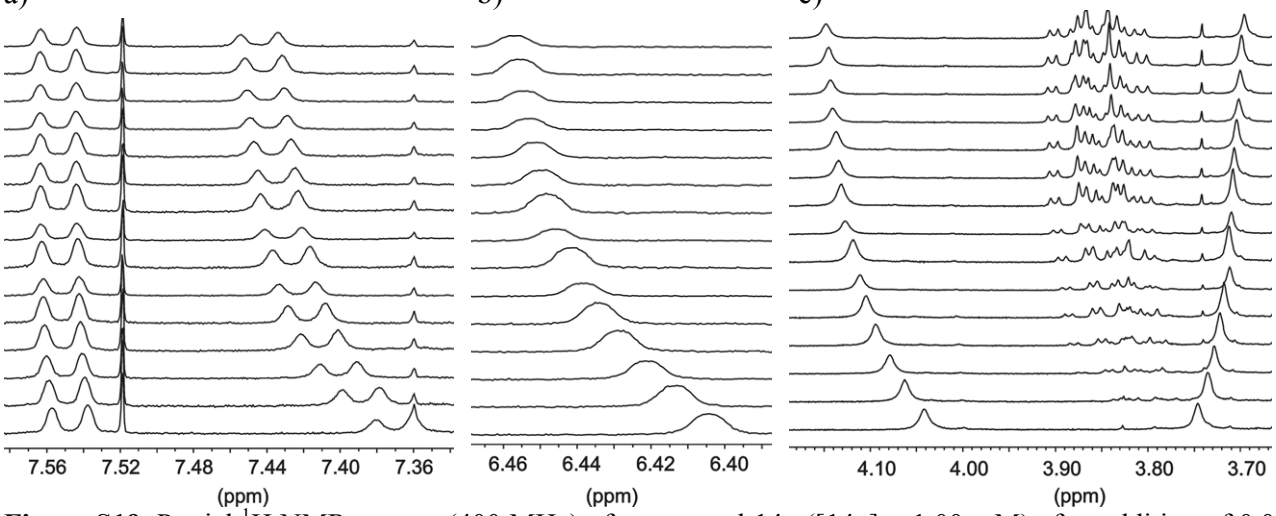

Figure S19. Partial ^{1}H NMR spectra (400 MHz) of compound **14a** ([**14a**] = 1.00 mM) after addition of 0.00 – 4.10 equiv of β-glucoside **27a** in $CDCl_3$. Shown are chemical shifts of the CH-indole (a) and CH_2 signals of **14a** (b,c).

3.2 ^{1}H NMR titrations of compound **14b** with β-glucoside **27a**.

a) b) c)

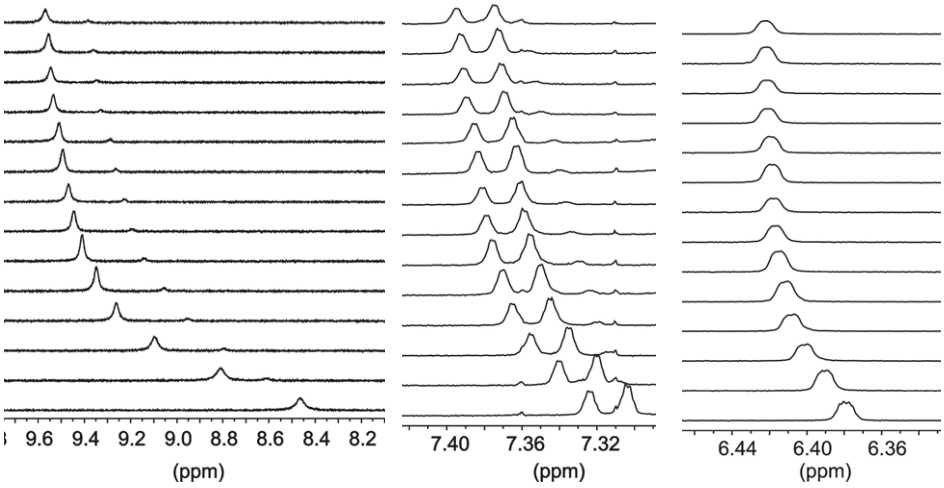

d)

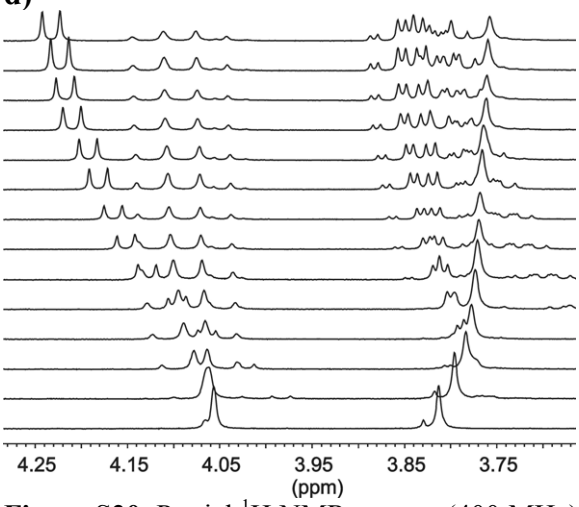

Figure S20. Partial ^{1}H NMR spectra (400 MHz) of compound **14b** ([**14b**] = 1.00 mM) after addition of 0.00 – 4.97 equiv of β-glucoside **27a** in $CDCl_3$. Shown are chemical shifts of the NH-indole (a), CH-indole (b,c) and CH_2 (d) signals of **14b**.

3.3 ^{1}H NMR titrations of compound **16a** with β-glucoside **27a**.

a) b) c)

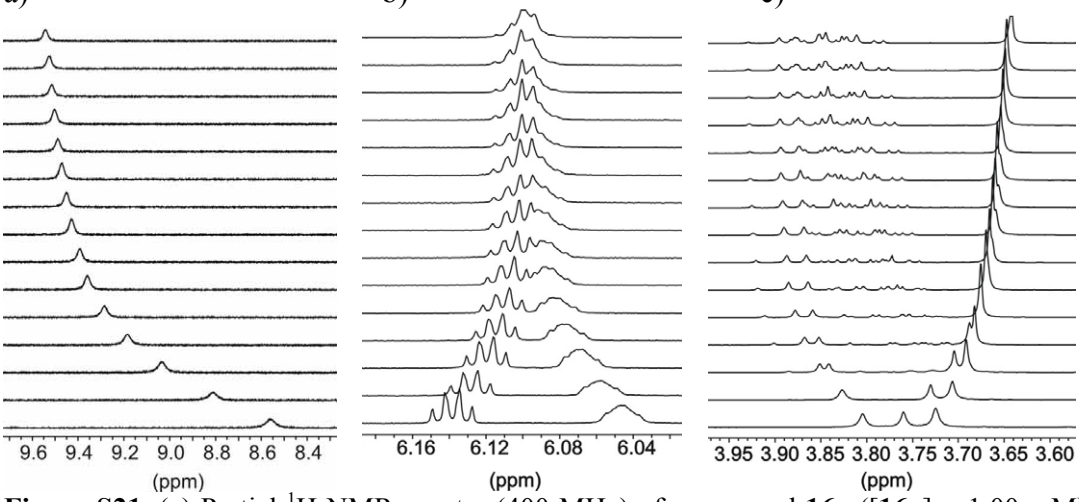

Figure S21. (a) Partial ^{1}H NMR spectra (400 MHz) of compound **16a** ([**16a**] = 1.00 mM) after addition of 0.00 – 5.01 equiv of β-glucoside **27a** in $CDCl_3$. Shown are chemical shifts of the NH-pyrrole (a), CH-pyrrole (b) and CH_2/OCH_3 (c) signals of **16a**.

3.4 ^{1}H NMR titrations of compound **16a** with β-galactoside **29a**.

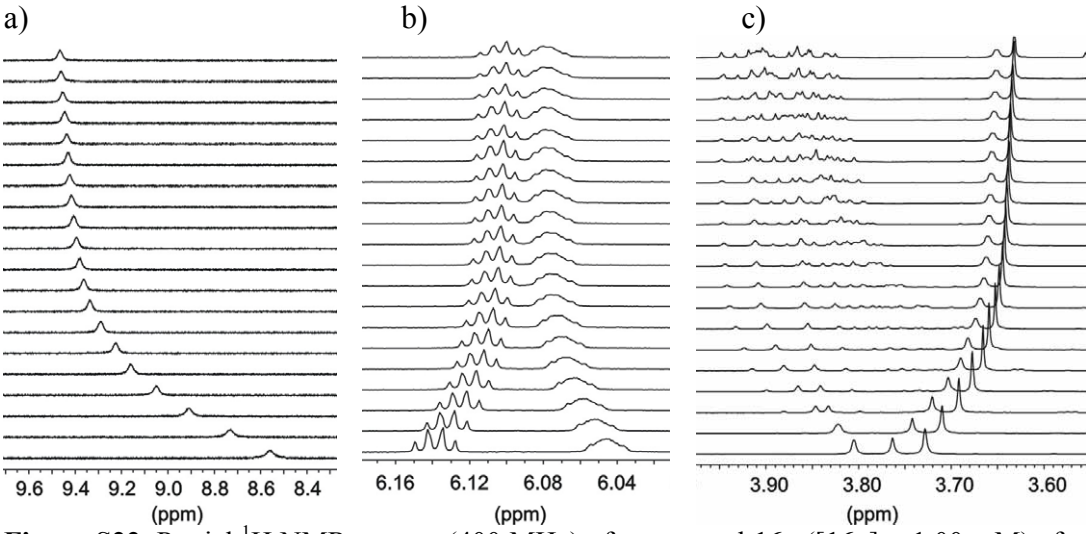

Figure S22. Partial ^{1}H NMR spectra (400 MHz) of compound **16a** ([**16a**] = 1.00 mM) after addition of 0.00 – 4.49 equiv of β-galactoside **29a** in $CDCl_3$. Shown are chemical shifts of the NH-pyrrole (a), CH-pyrrole (b) and CH_2/OCH_3 (c) signals of **16a**.

3.5 ^{1}H NMR titrations of compound **16b** with β-glucoside **27a**.

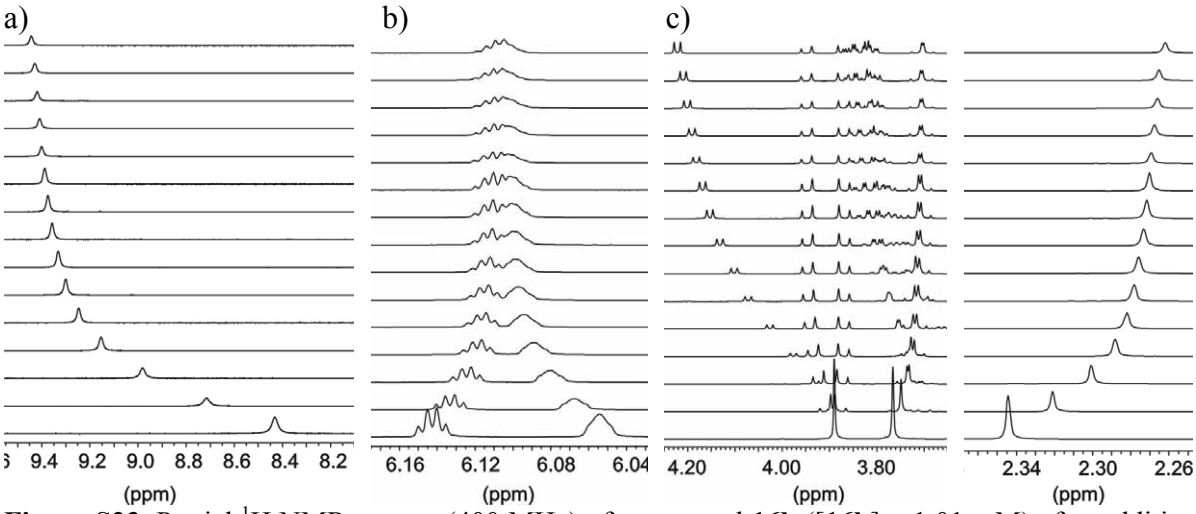

Figure S23. Partial ^{1}H NMR spectra (400 MHz) of compound **16b** ([**16b**] = 1.01 mM) after addition of 0.00 – 4.98 equiv of β-glucoside **27a** in $CDCl_3$. Shown are chemical shifts of the NH-pyrrole (a), CH-pyrrole (b) and CH_2/OCH_3 (c) signals of **16b**.

3.6 ^{1}H NMR titrations of compound **16b** with β-galactoside **29a**.

a) b) c)

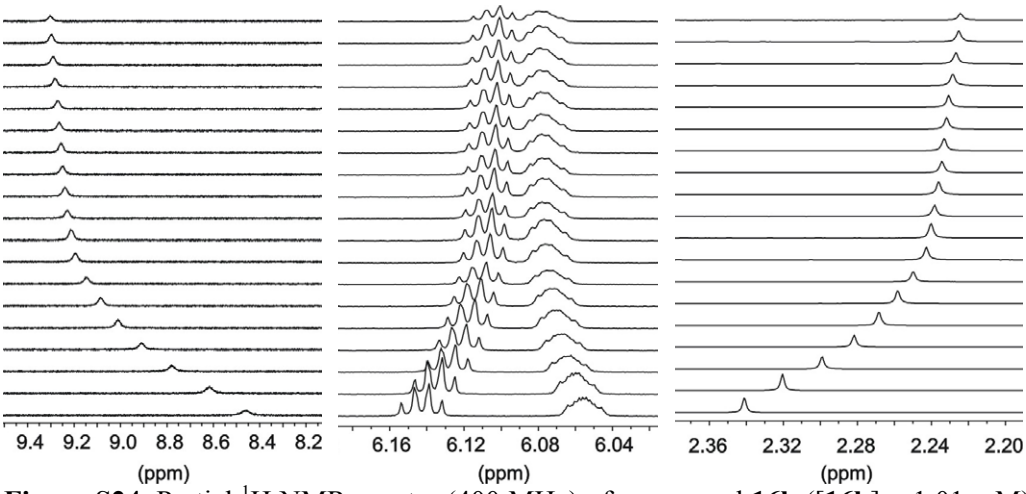

Figure S24. Partial ^{1}H NMR spectra (400 MHz) of compound **16b** ([**16b**] = 1.01 mM) after addition of 0.00 – 4.49 equiv of β-galactoside **29a** in $CDCl_3$. Shown are chemical shifts of the NH-pyrrole (a), CH-pyrrole (b) and OCH_3 (c) signals of **16b**.

3.7 ^{1}H NMR titrations of compound **14a** with α-galactoside **30a**.

a) b)

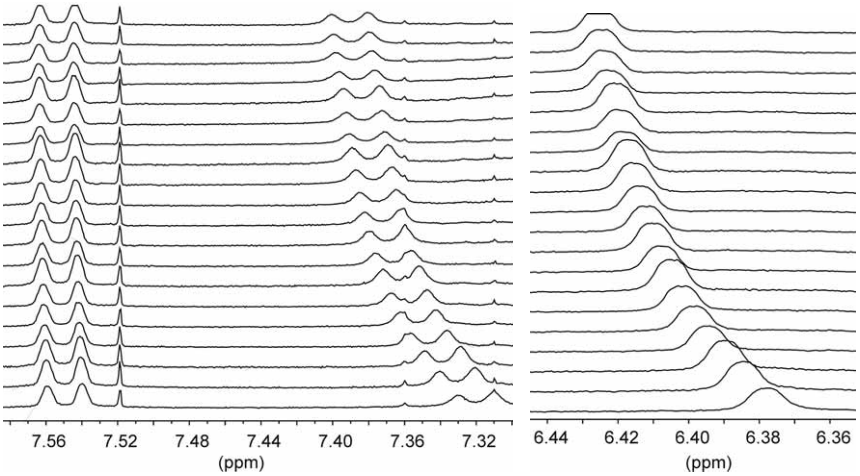

c)

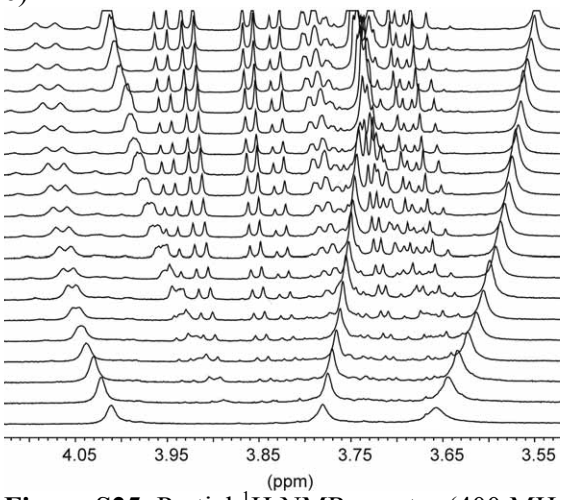

Figure S25. Partial ^{1}H NMR spectra (400 MHz) of compound **14a** ([**14a**] = 1.00 mM) after addition of 0.00 – 4.51 equiv of α-galactoside **30a** in $CDCl_3$. Shown are chemical shifts of the CH-indole (a,b), CH_2 and OCH_3 (c) signals of **14a**.

3.8 ^{1}H NMR titrations of compound **15a** with β-glucoside **27a**.

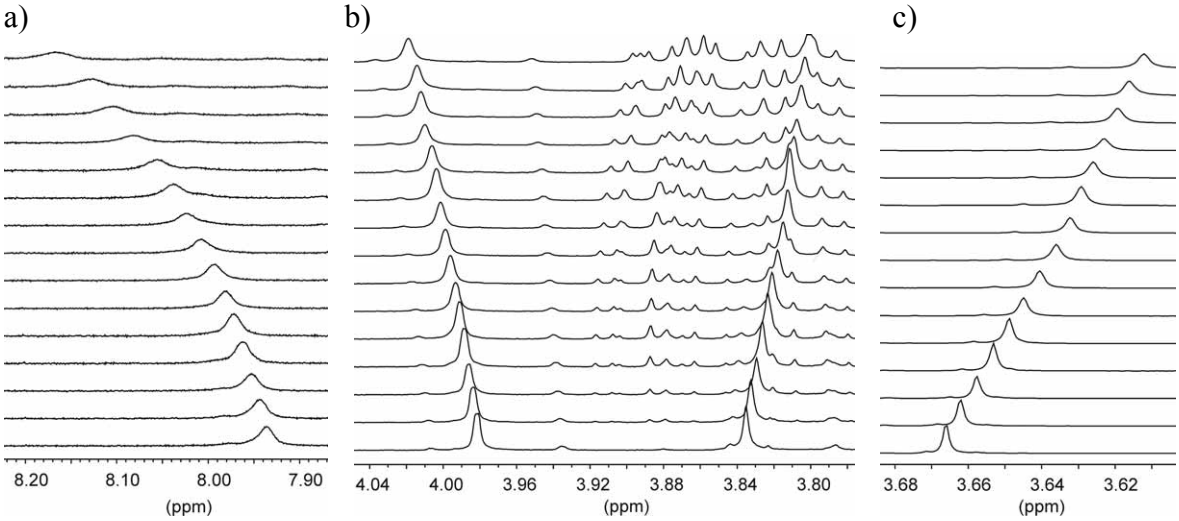

Figure S26. Partial ^{1}H NMR spectra (400 MHz) of compound **15a** ([**15a**] = 1.01 mM) after addition of 0.00 – 4.08 equiv of β-glucoside **27a** in $CDCl_3$. Shown are chemical shifts of the NH- (a), CH_2 (b) and OCH_3 (c) signals of **15a**.

3.9 ^{1}H NMR titrations of compound **16a** with α-galactoside **30a**.

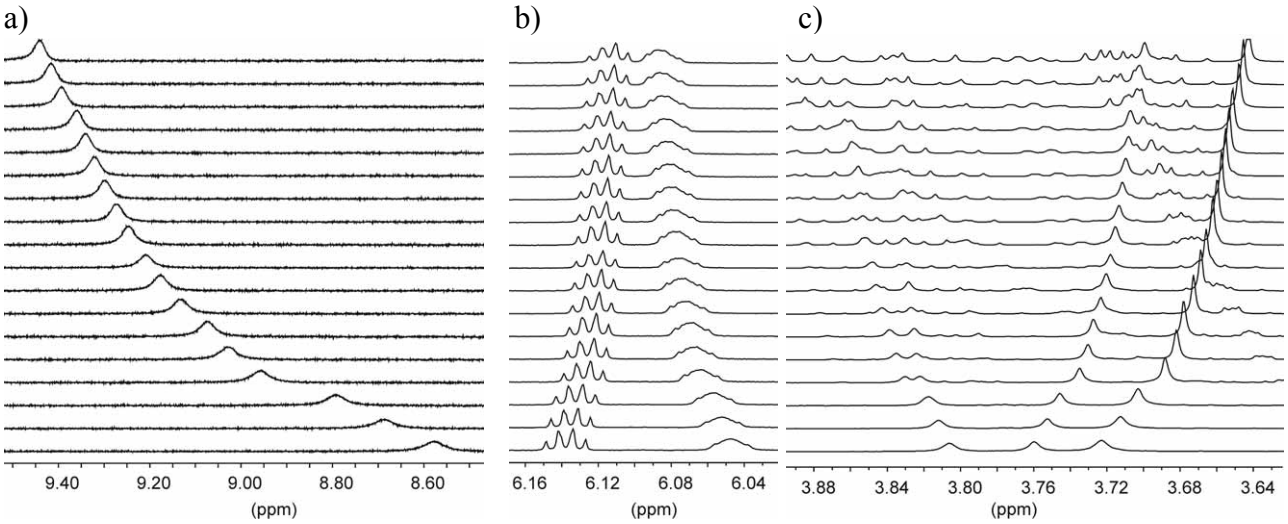

Figure S27. Partial ^{1}H NMR spectra (400 MHz) of compound **16a** ([**16a**] = 1.00 mM) after addition of 0.00 – 5.01 equiv of α-galactoside **30a** in $CDCl_3$. Shown are chemical shifts of the NH- (a) , CH-pyrrole (b) , CH_2 and OCH_3 (c) signals of **16a**.

4 ^{1}H and ^{13}C NMR spectra of imidazole-, indole- and pyrrole-based compounds **12a**/**b**-**16a**/**b**.

4.1 ^{1}H and ^{13}C NMR spectra of compound **12a**.

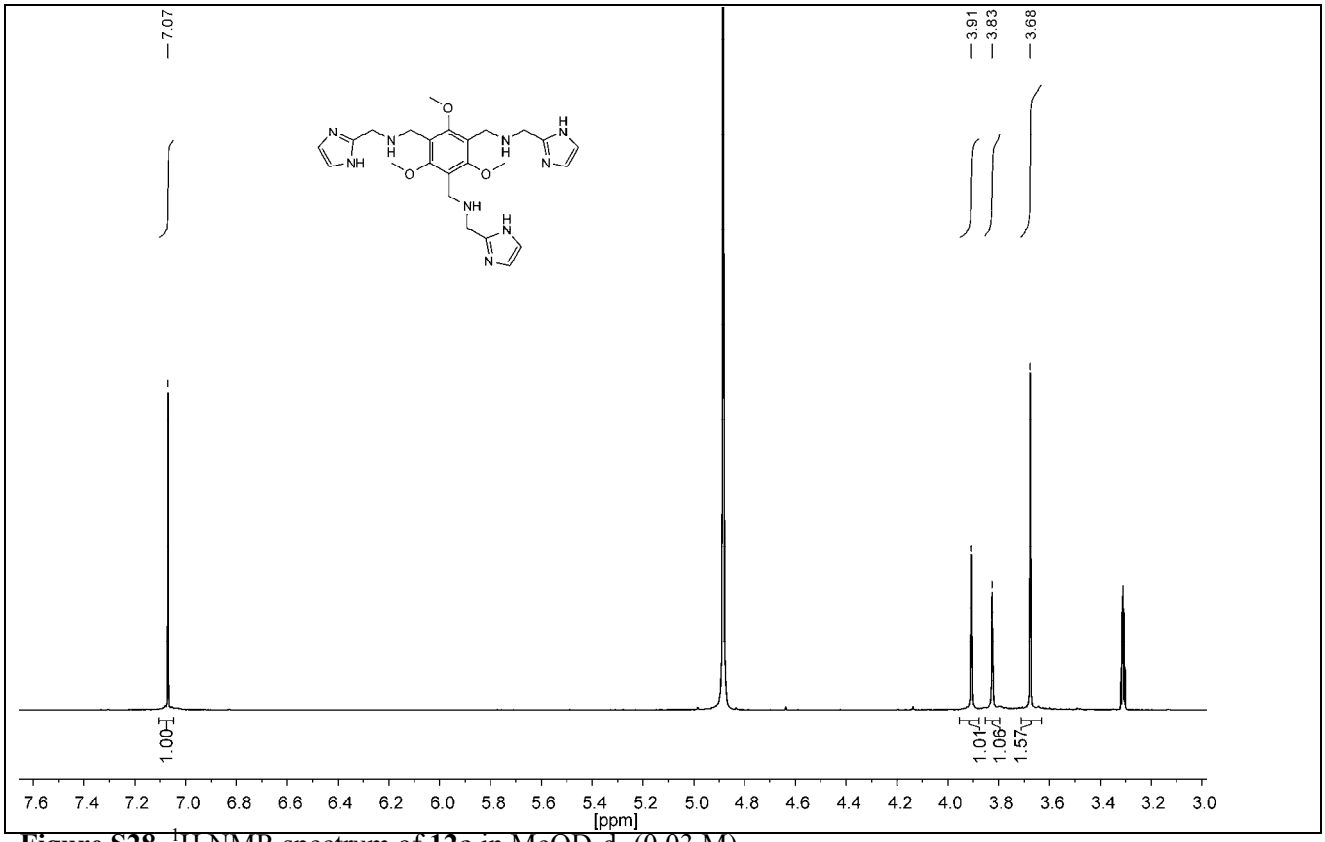

Figure S28. ^{1}H NMR spectrum of **12a** in MeOD-d_4 (0.03 M).

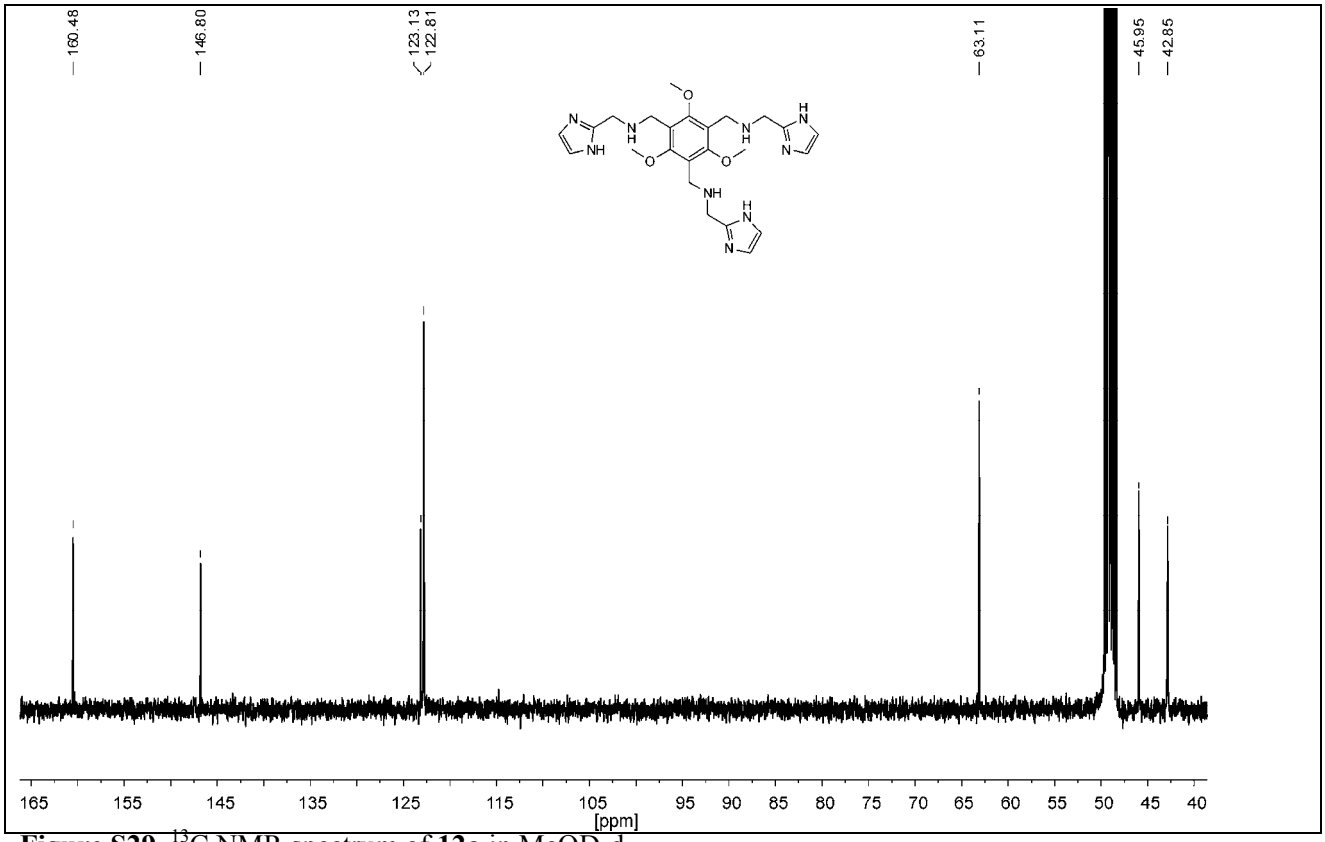

Figure S29. ^{13}C NMR spectrum of **12a** in MeOD-d_4.

4.2 ^{1}H and ^{13}C NMR spectra of compound **13a.**

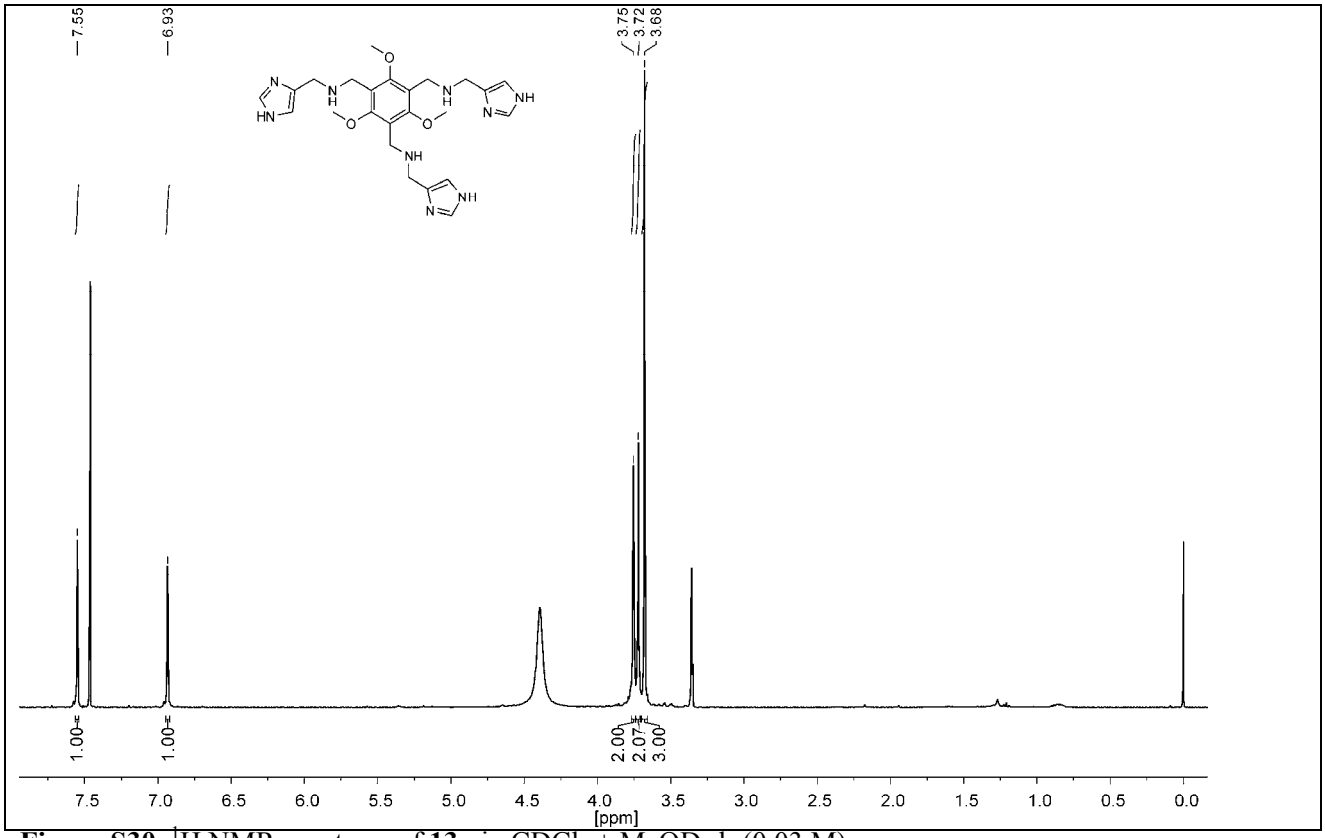

Figure S30. ^{1}H NMR spectrum of **13a** in $CDCl_3$ + MeOD-d_4 (0.03 M).

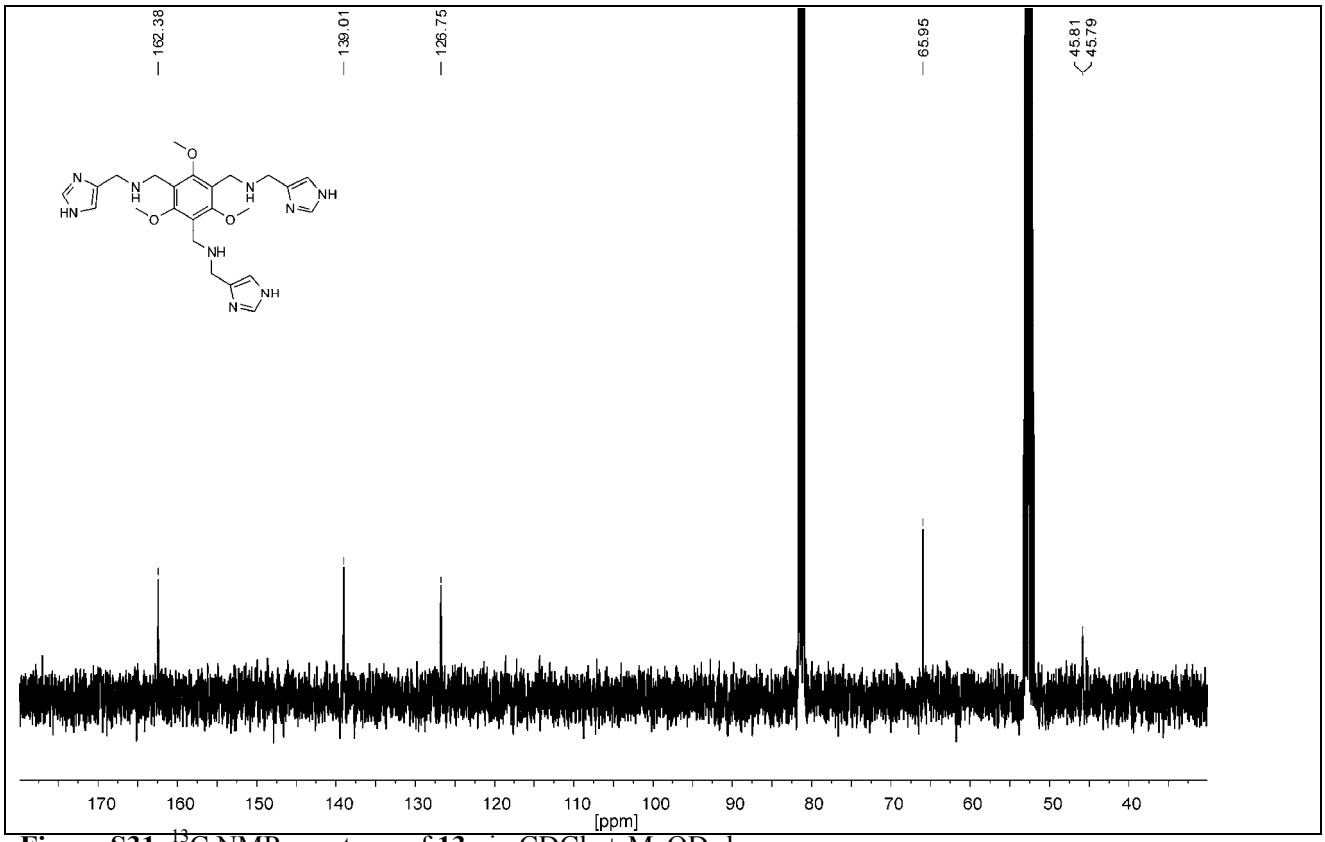

Figure S31. ^{13}C NMR spectrum of **13a** in $CDCl_3$ + MeOD-d_4.

4.3 ^{1}H and ^{13}C NMR spectra of compound **14a.**

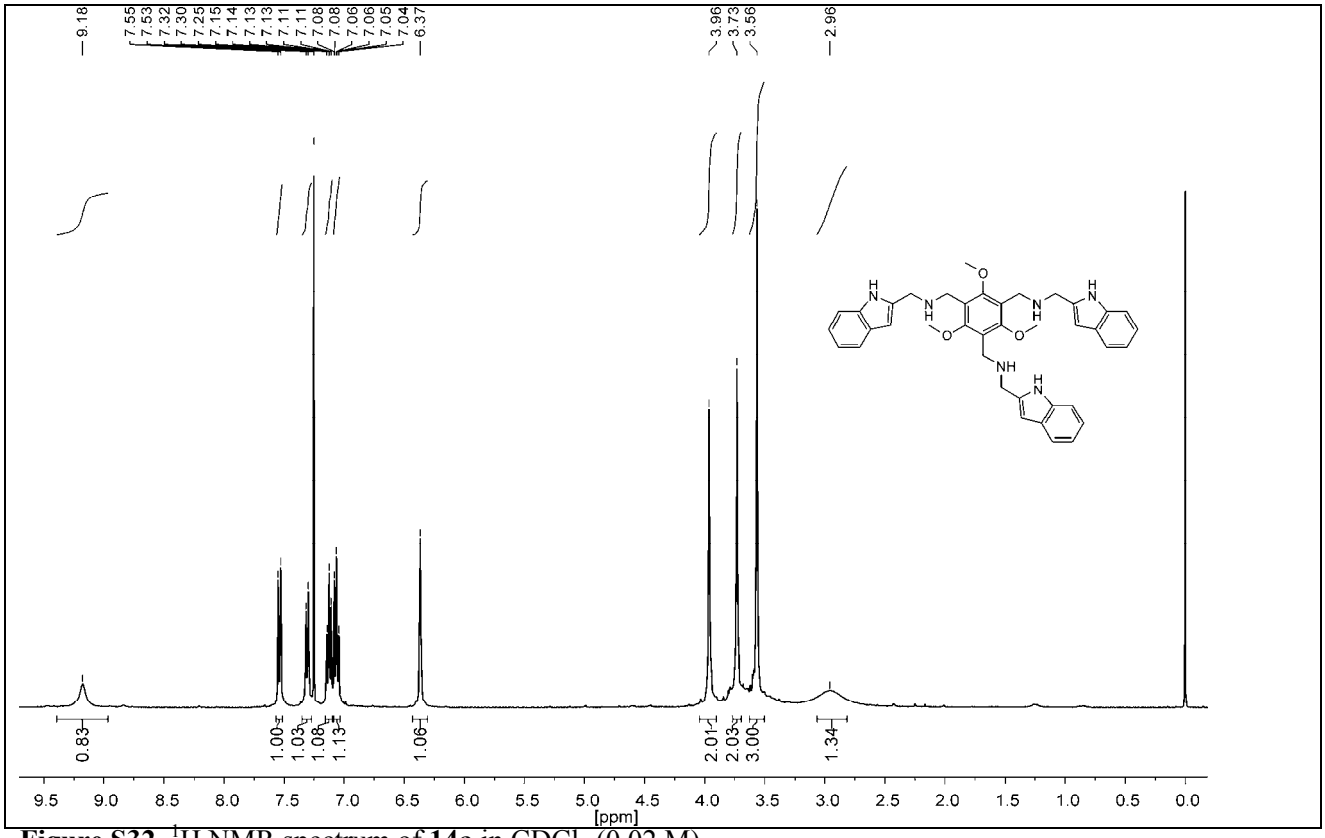

Figure S32. ^{1}H NMR spectrum of **14a** in $CDCl_3$ (0.02 M).

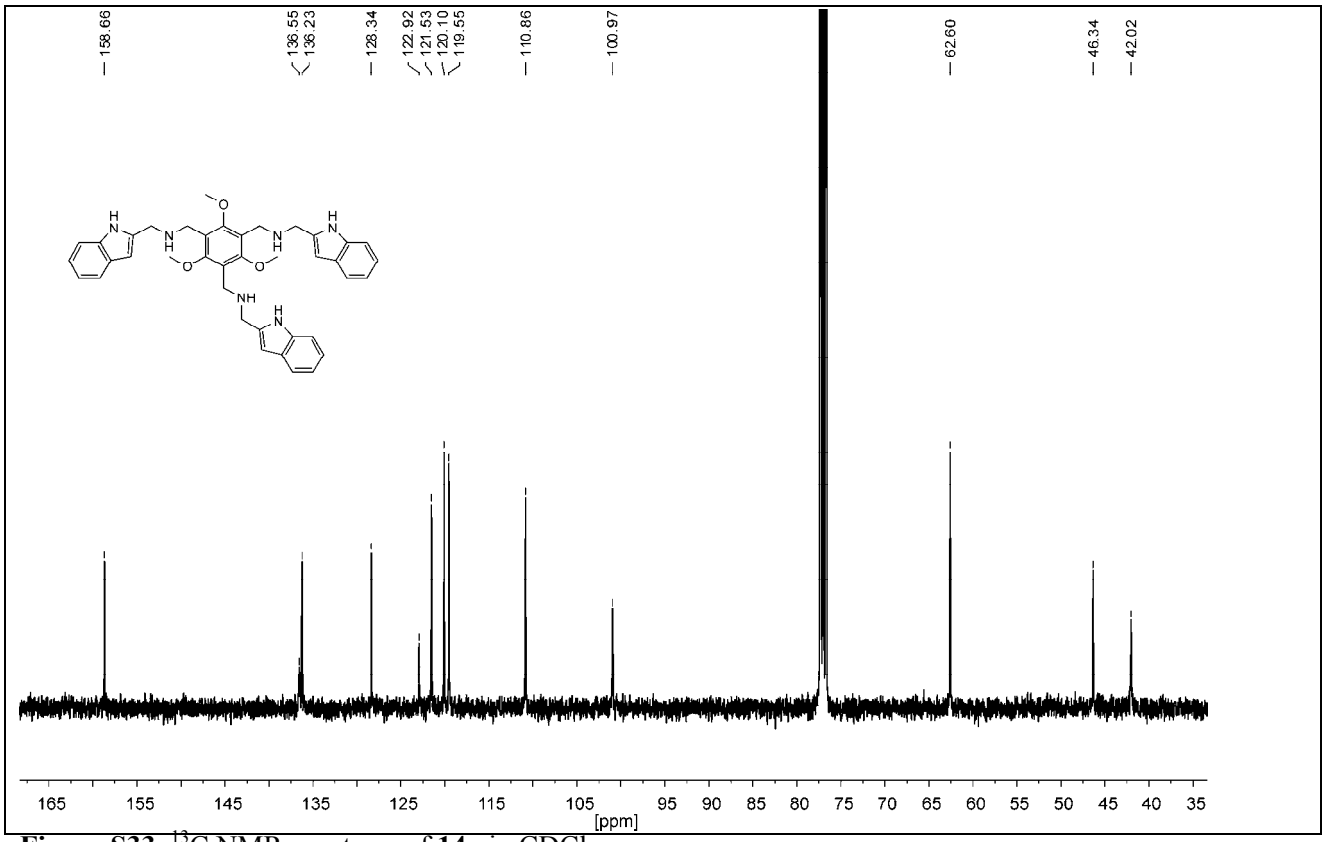

Figure S33. ^{13}C NMR spectrum of **14a** in $CDCl_3$.

4.4 ^{1}H and ^{13}C NMR spectra of compound **15a**.

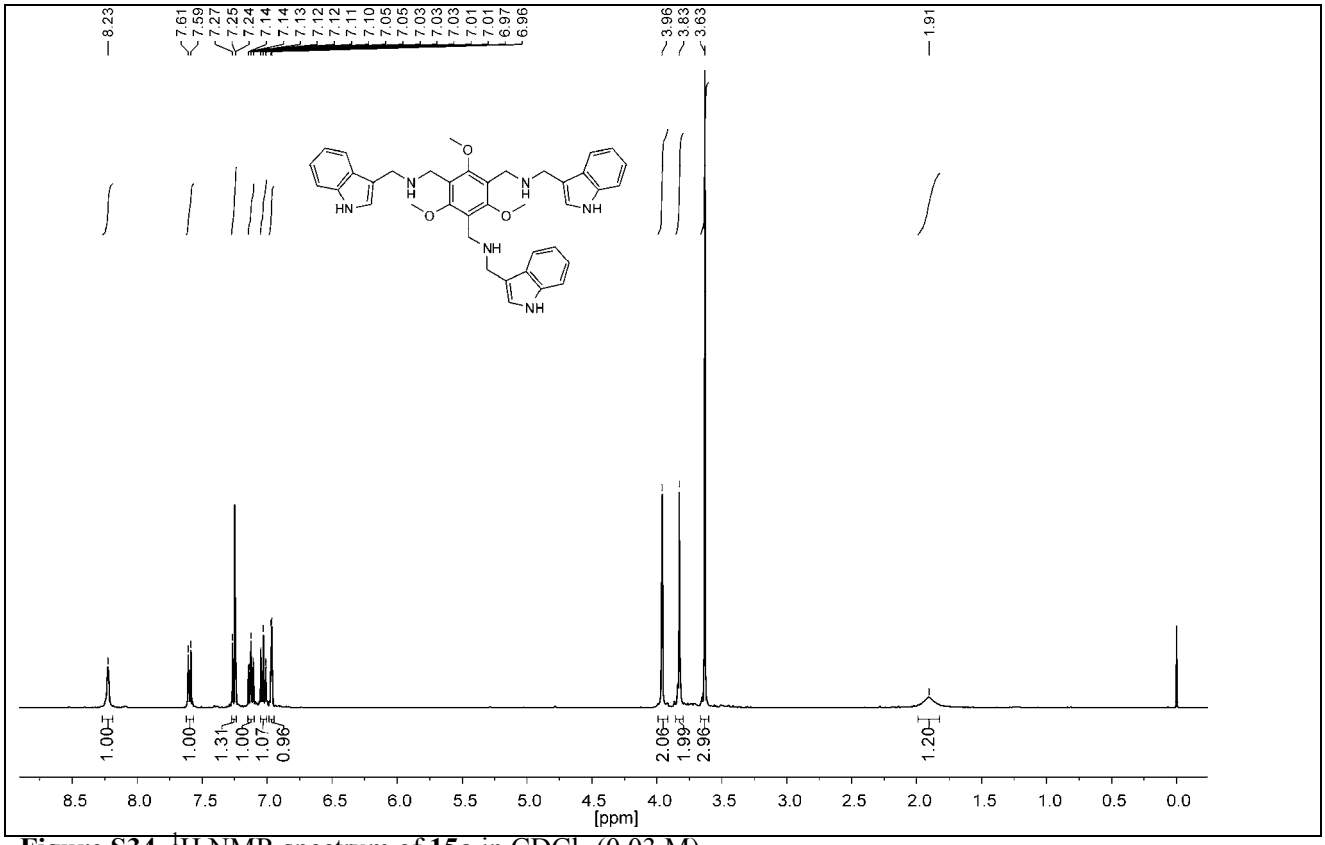

Figure S34. ^{1}H NMR spectrum of **15a** in $CDCl_3$ (0.03 M).

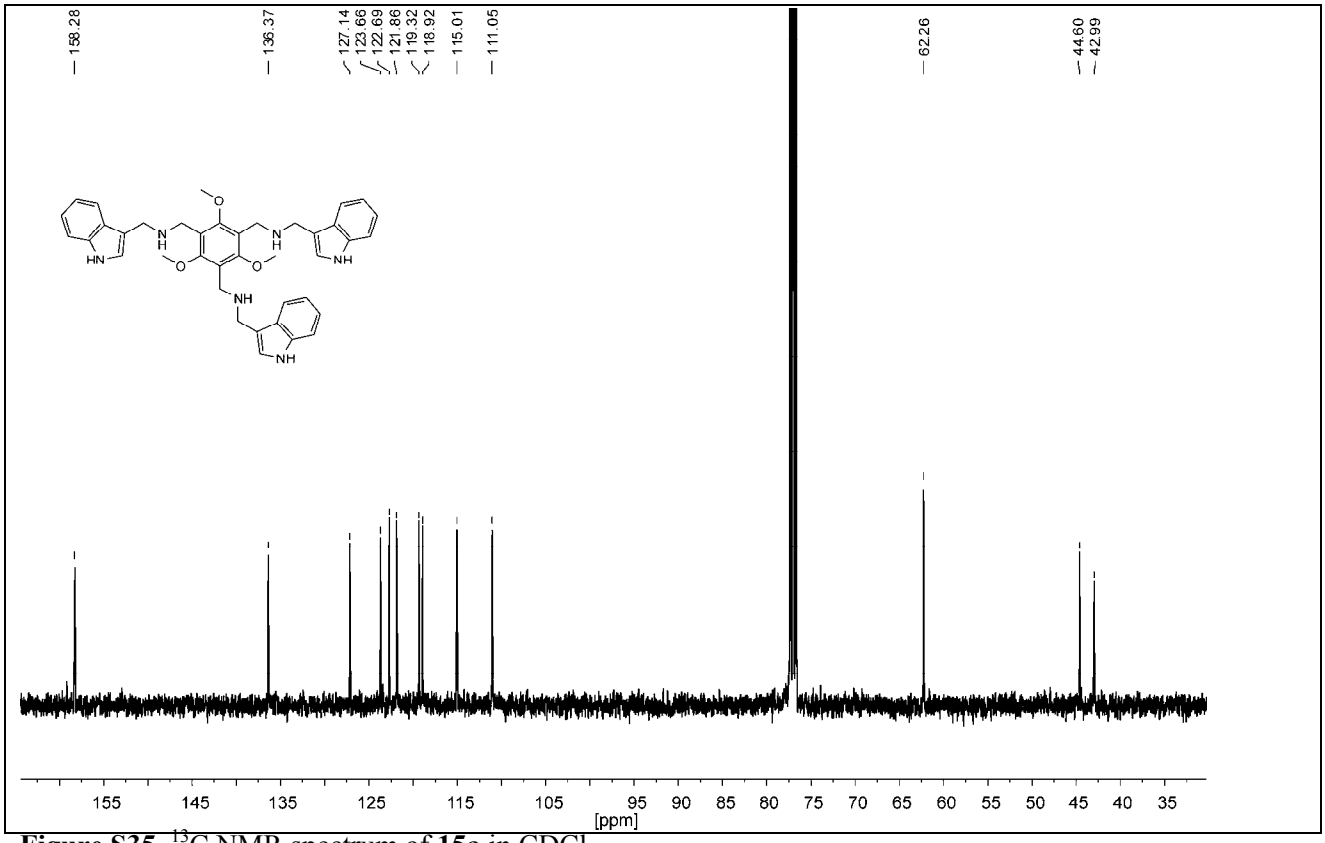

Figure S35. ^{13}C NMR spectrum of **15a** in $CDCl_3$.

4.5 ^{1}H and ^{13}C NMR spectra of compound **16a.**

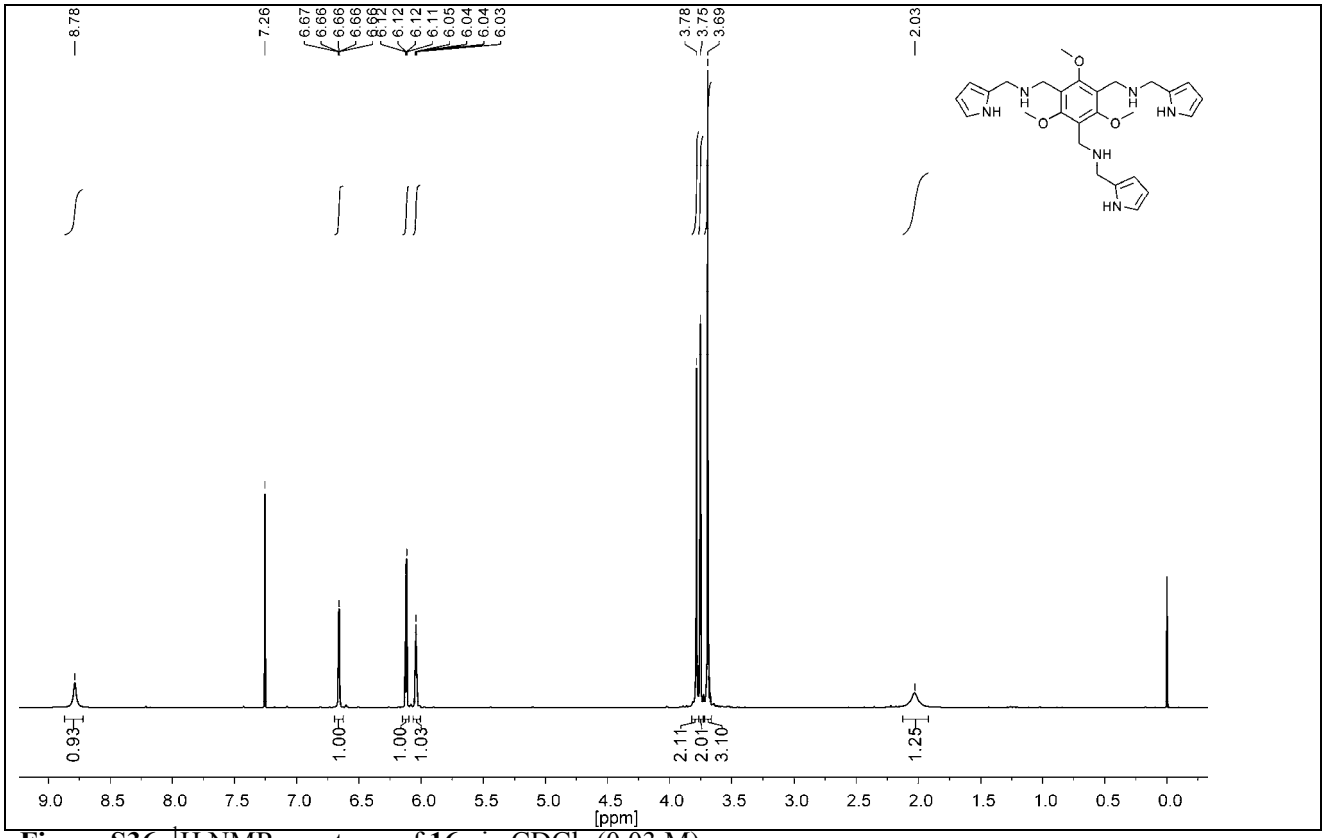

Figure S36. ^{1}H NMR spectrum of **16a** in $CDCl_3$ (0.03 M).

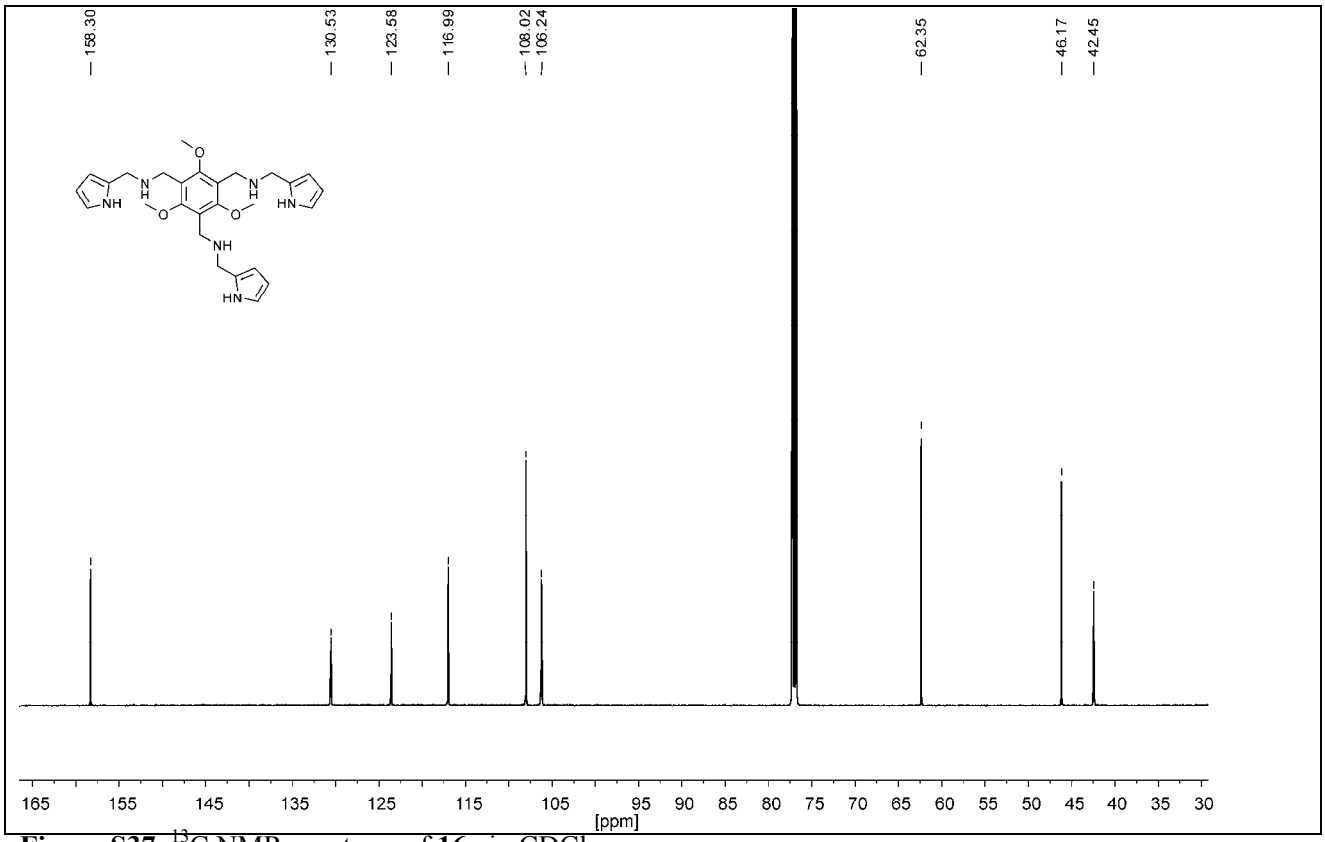

Figure S37. ^{13}C NMR spectrum of **16a** in $CDCl_3$.

4.6 ^{1}H and ^{13}C NMR spectra of compound **12b**.

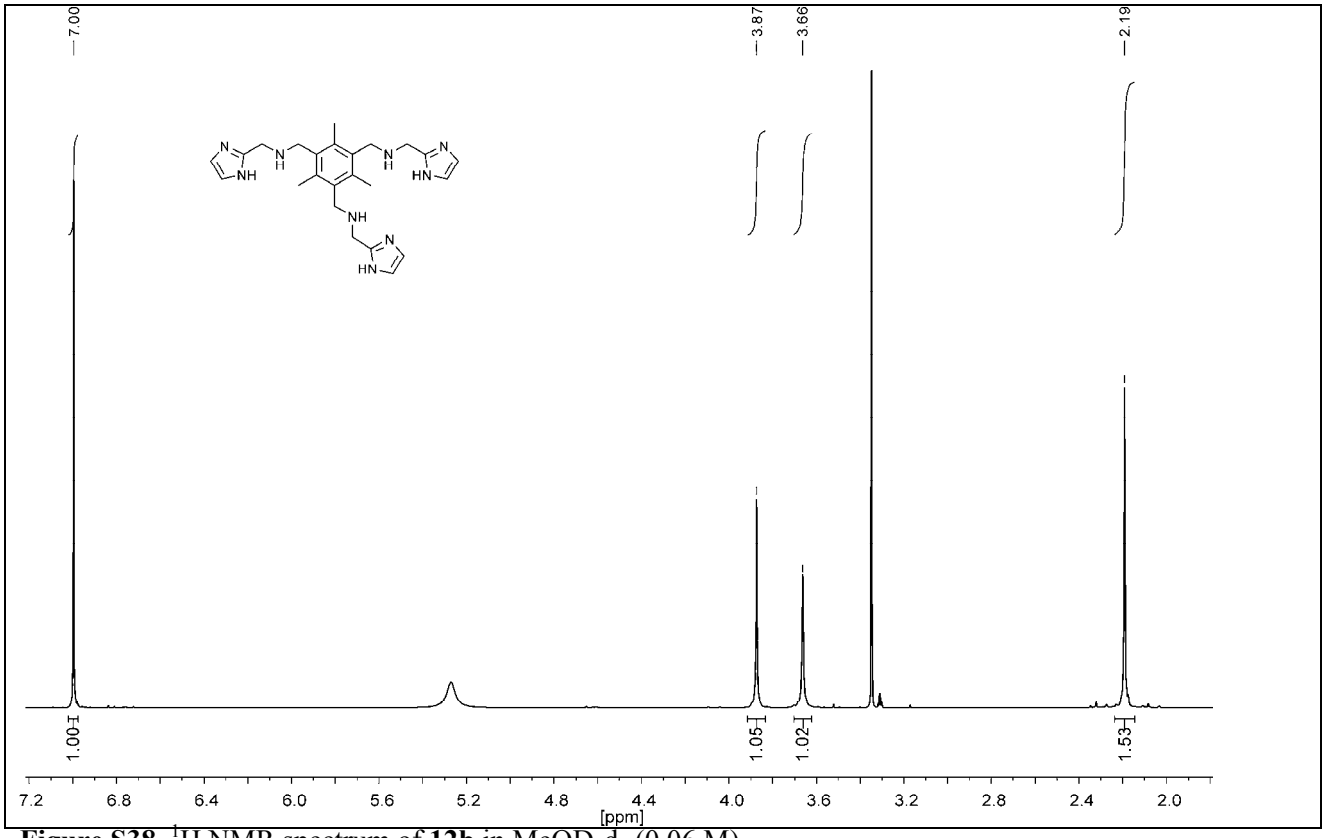

Figure S38. ^{1}H NMR spectrum of **12b** in MeOD-d_4 (0.06 M).

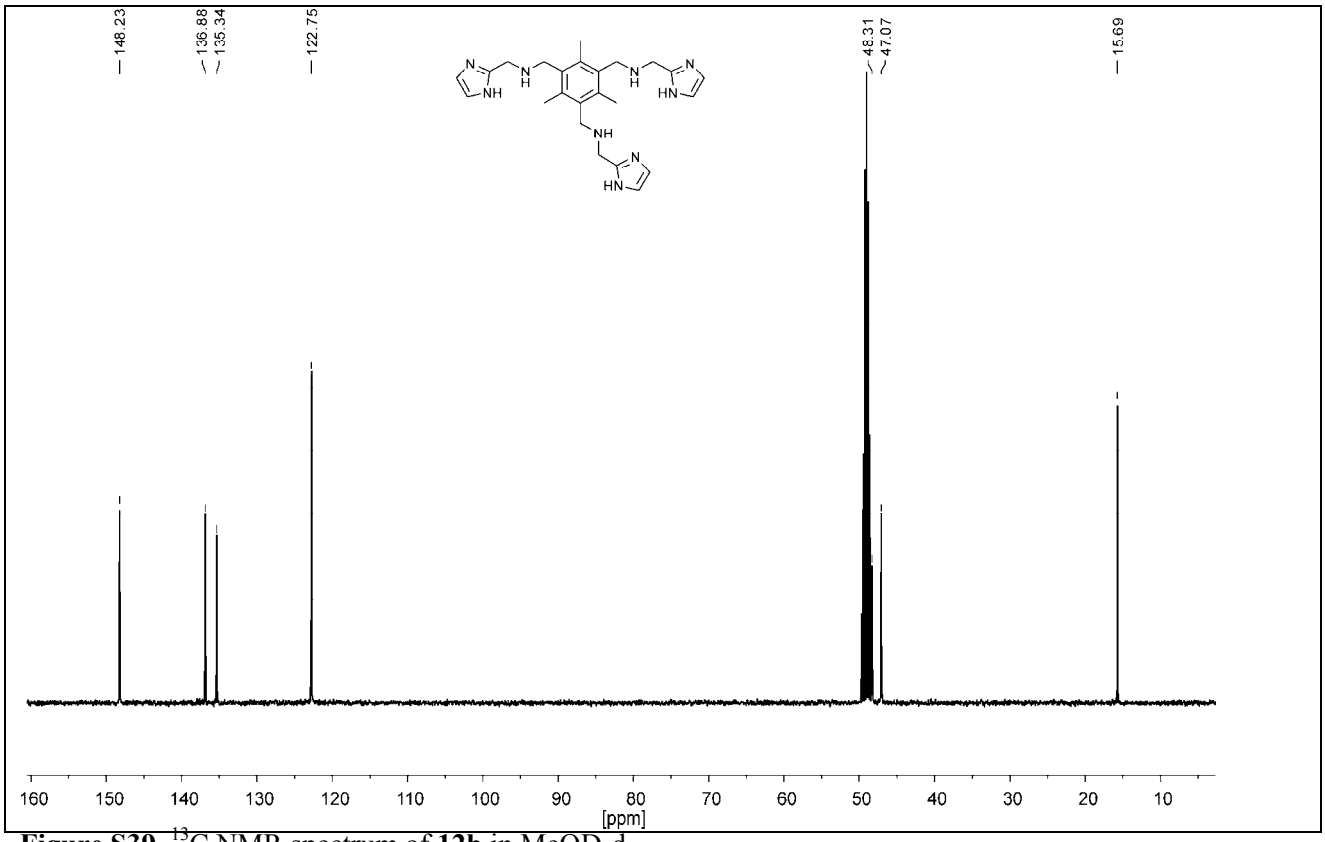

Figure S39. ^{13}C NMR spectrum of **12b** in MeOD-d_4.

4.7 ^{1}H and ^{13}C NMR spectra of compound **13b**.

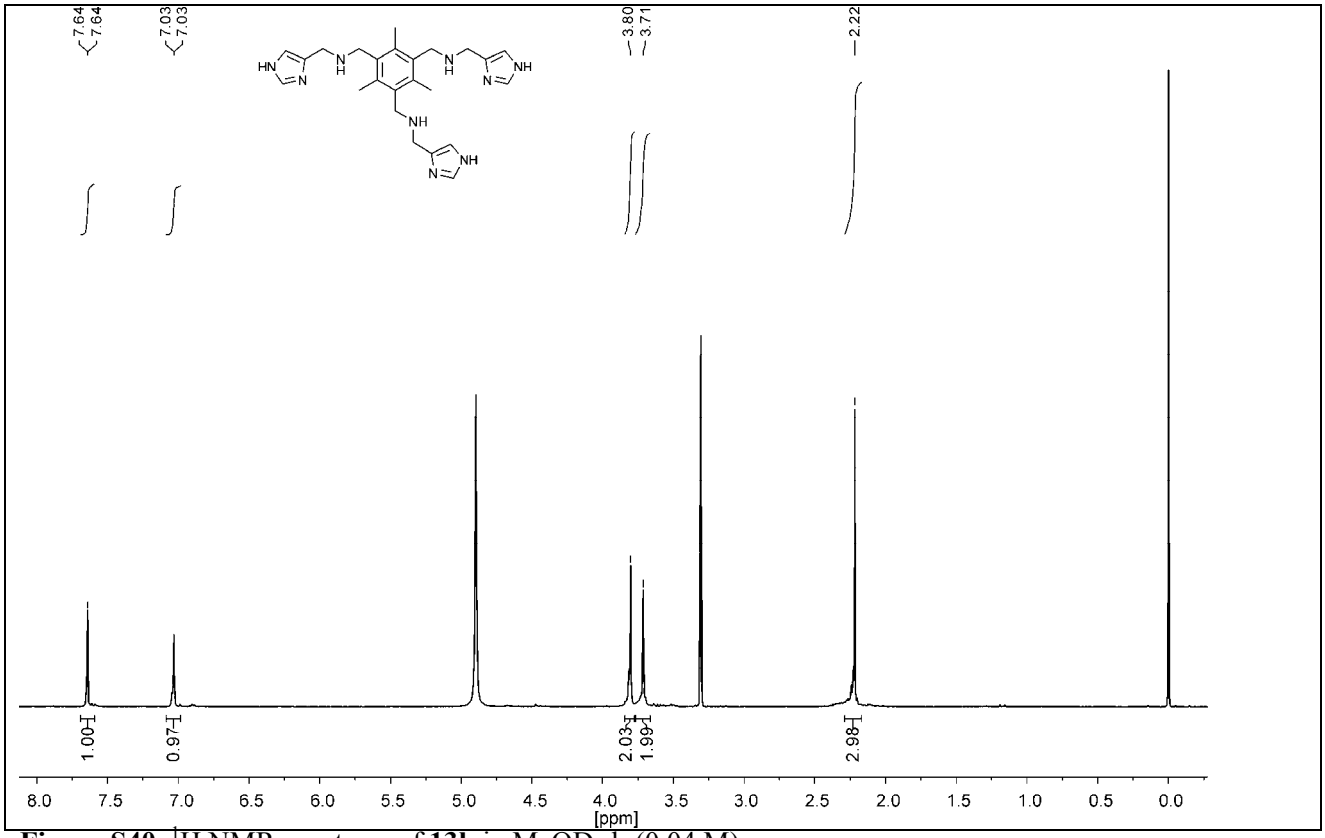

Figure S40. ^{1}H NMR spectrum of **13b** in MeOD-d_4 (0.04 M).

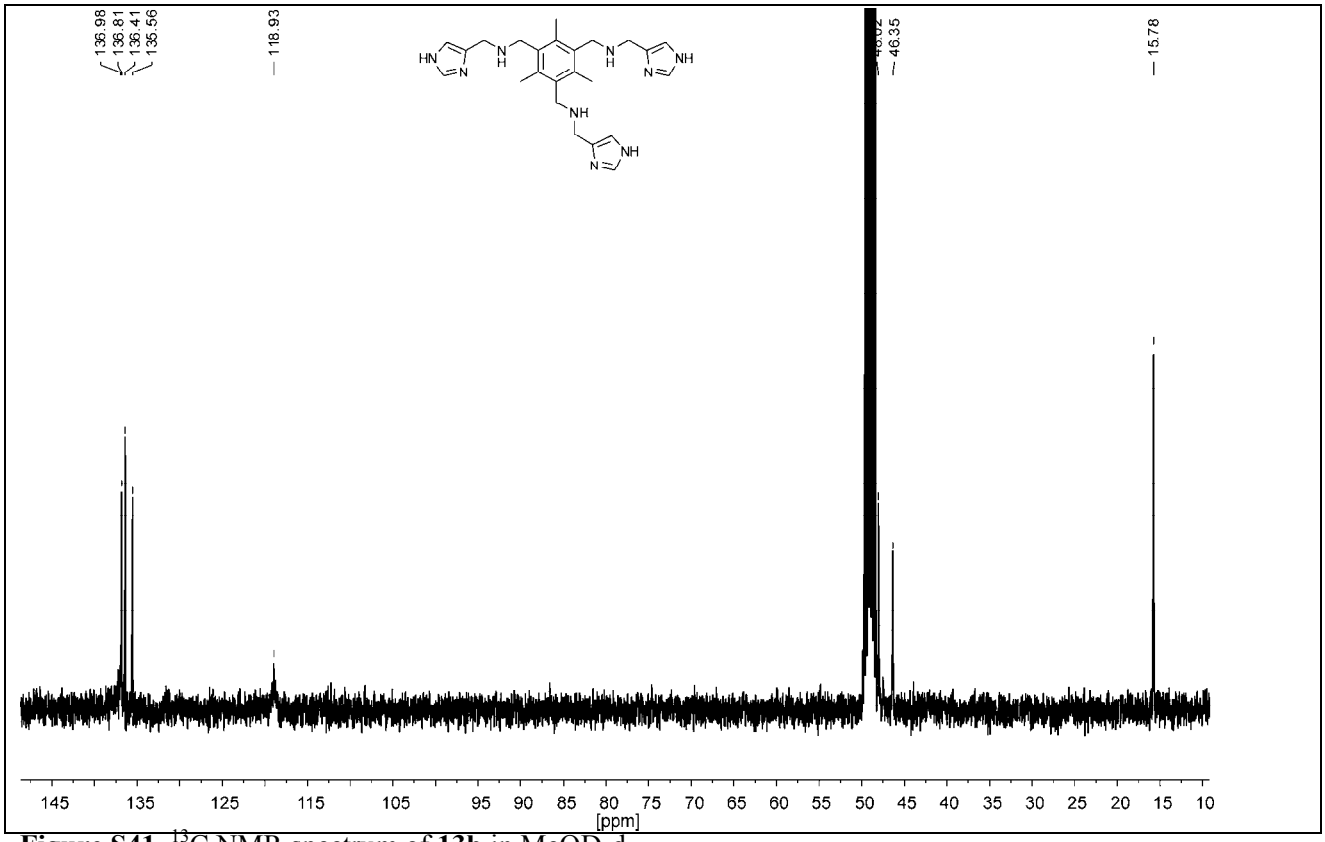

Figure S41. ^{13}C NMR spectrum of **13b** in MeOD-d_4.

4.8 ^{1}H and ^{13}C NMR spectra of compound **14b**.

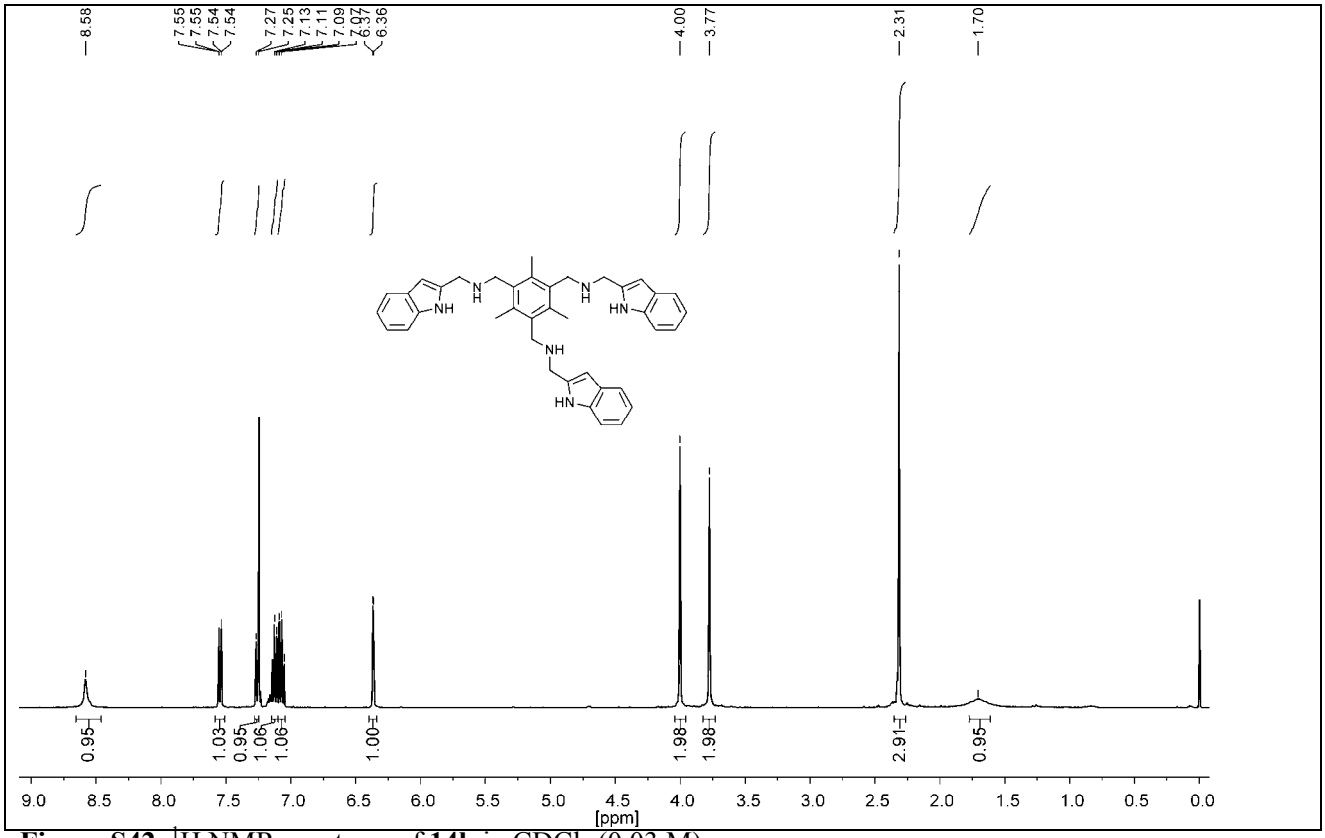

Figure S42. ^{1}H NMR spectrum of **14b** in $CDCl_3$ (0.03 M).

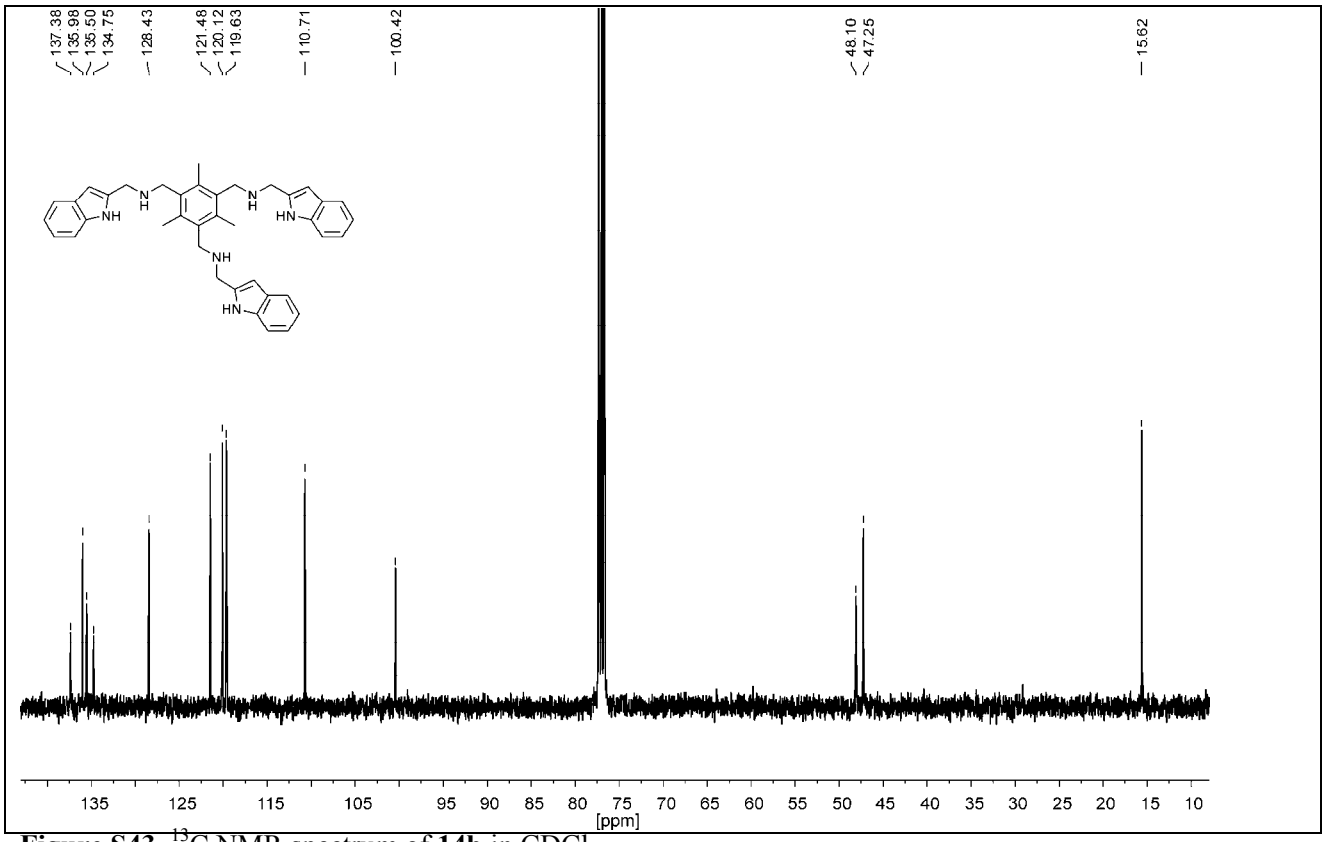

Figure S43. ^{13}C NMR spectrum of **14b** in $CDCl_3$.

4.9 ^{1}H and ^{13}C NMR spectra of compound **15b**.

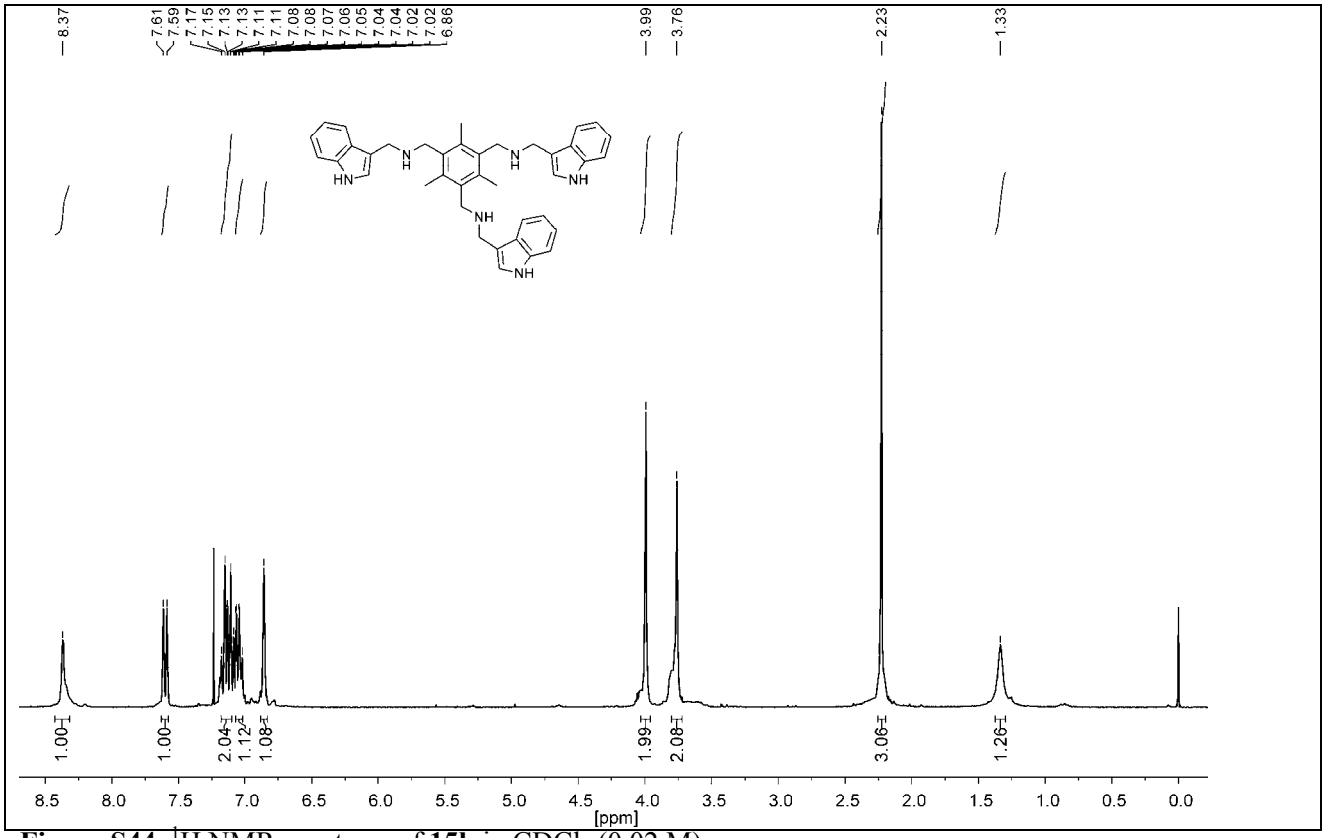

Figure S44. ^{1}H NMR spectrum of **15b** in $CDCl_3$ (0.02 M).

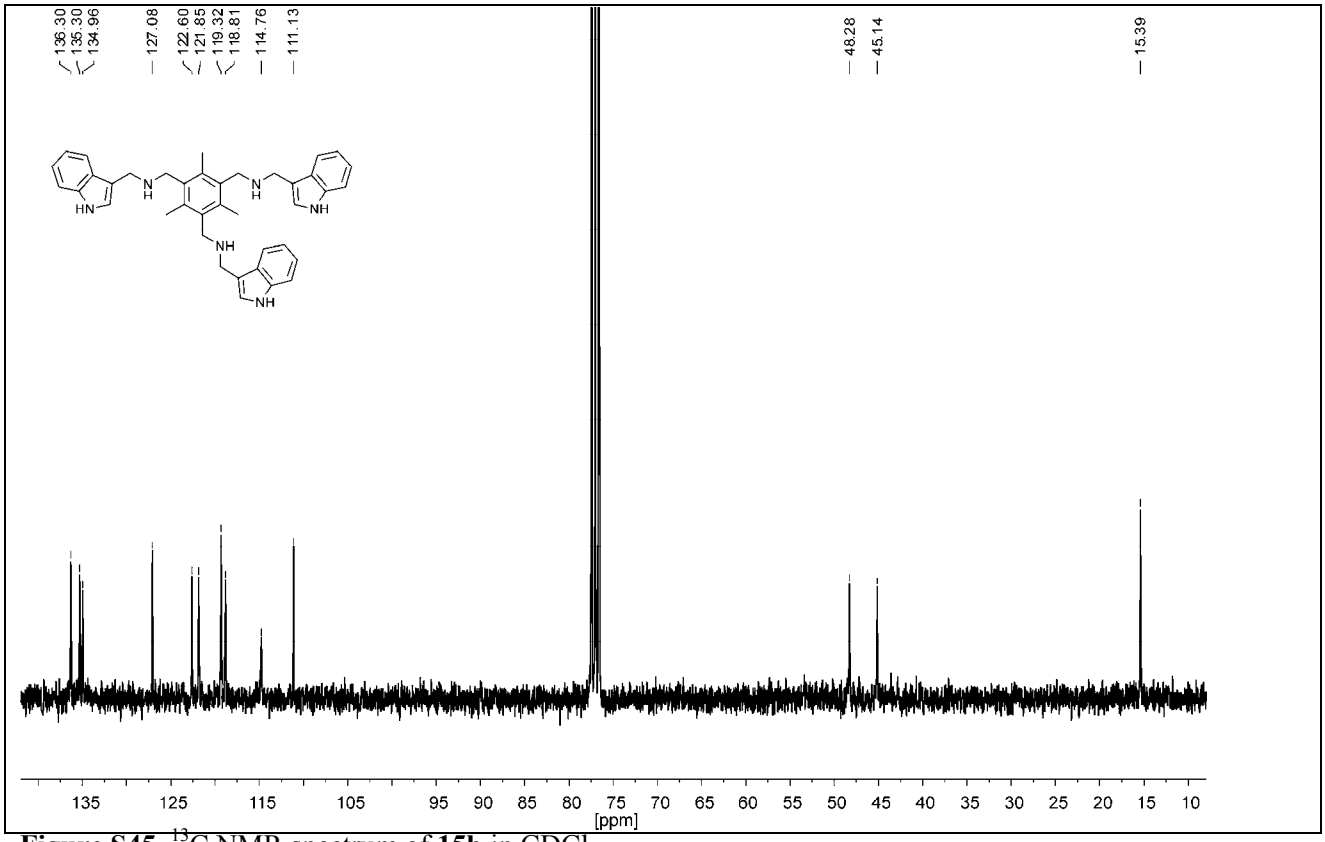

Figure S45. ^{13}C NMR spectrum of **15b** in $CDCl_3$.

4.10 ^{1}H and ^{13}C NMR spectra of compound **16b**.

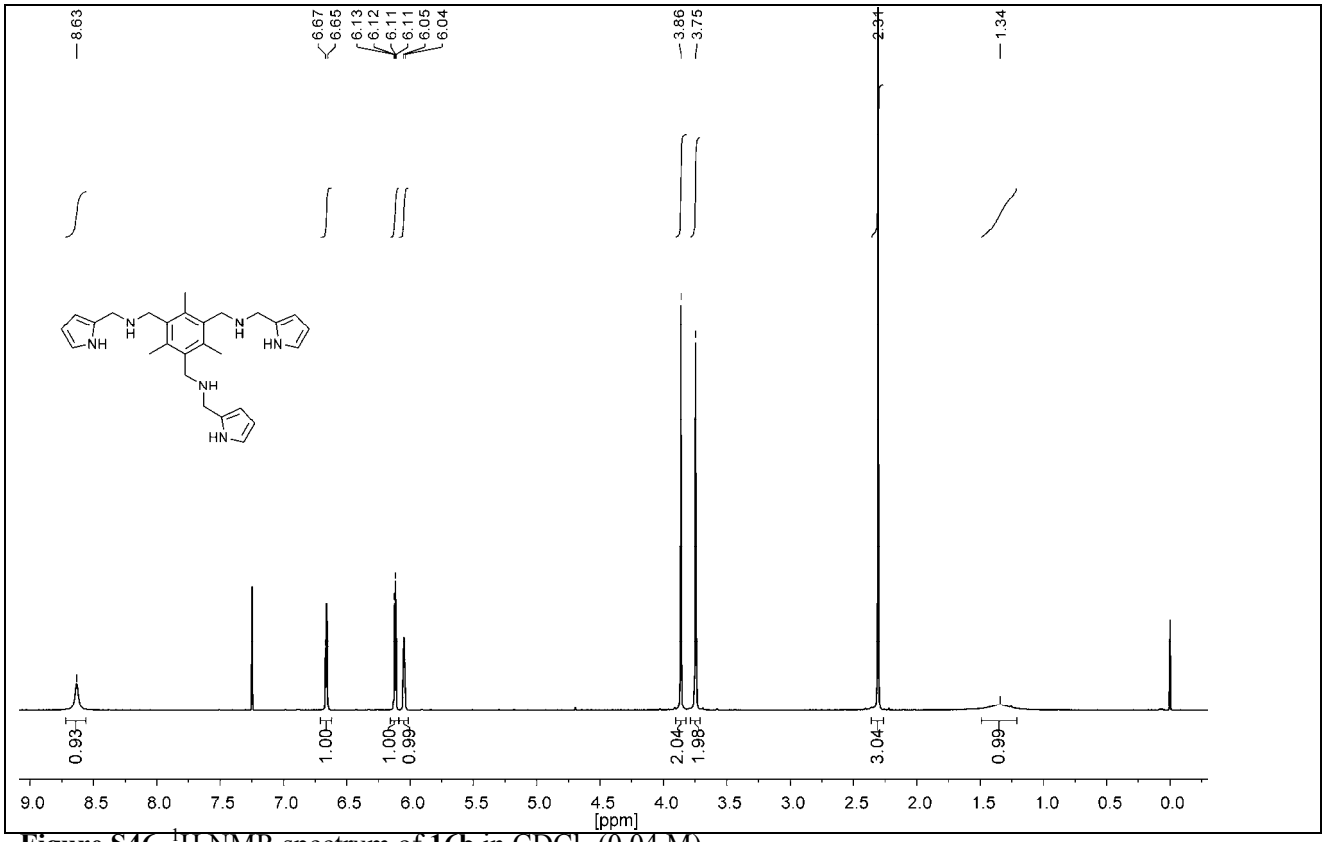

Figure S46. ^{1}H NMR spectrum of **16b** in $CDCl_3$ (0.04 M).

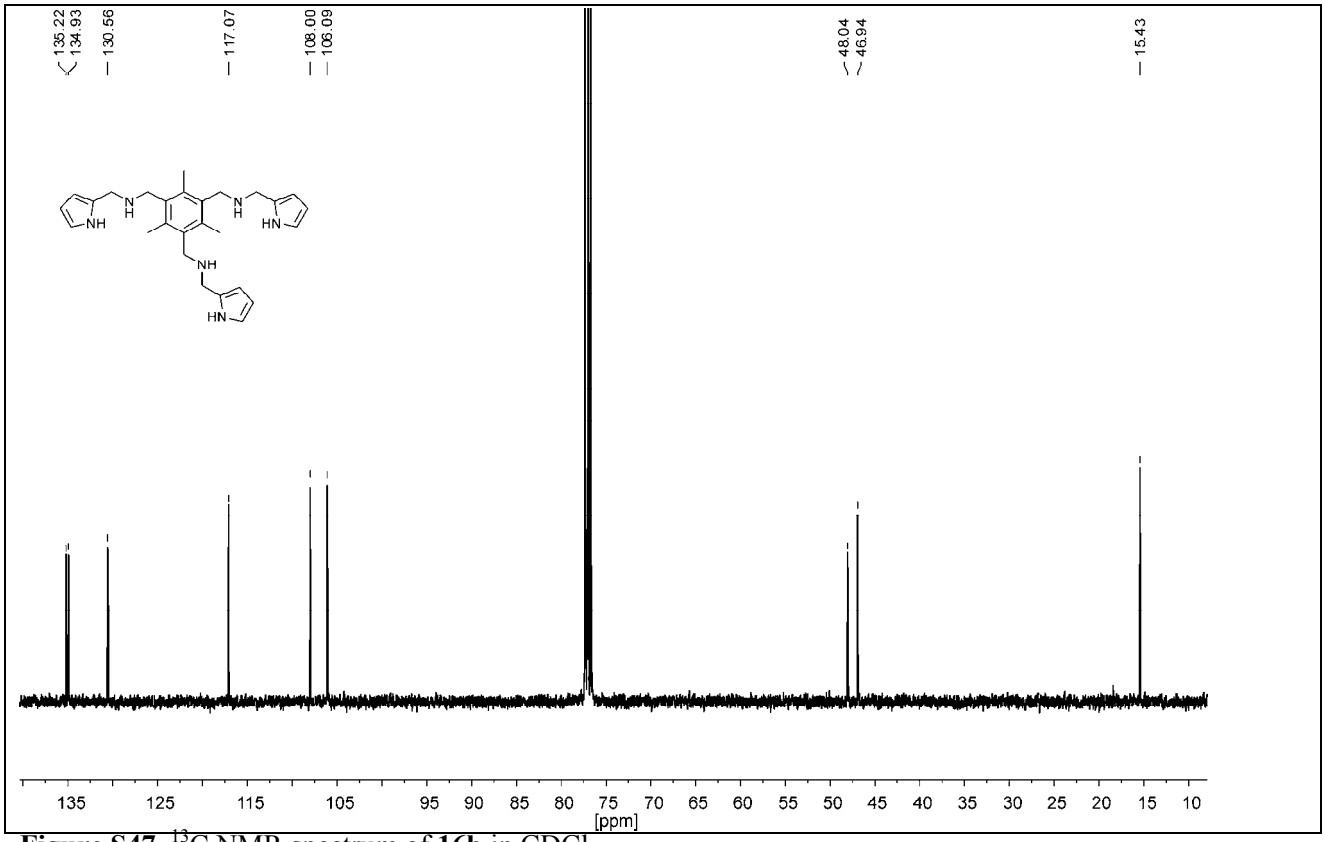

Figure S47. ^{13}C NMR spectrum of **16b** in $CDCl_3$.

5 Partial ^{1}H and ^{13}C NMR spectra of compound **14a** and **14b** (chemical shifts of the amine-NH signals of the two compounds)

a) b)

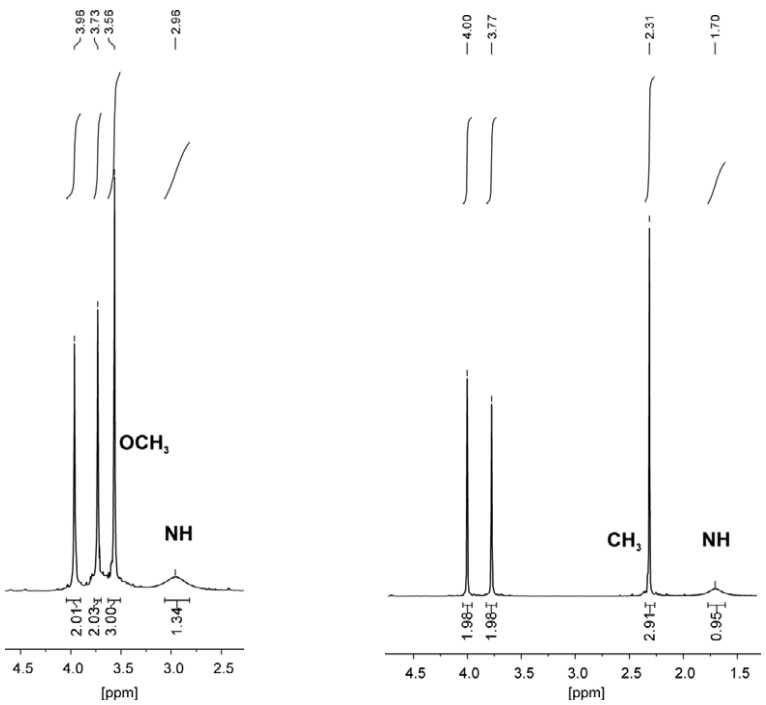

Figure 48. Partial ^{1}H NMR spectra (400 MHz) of compound **14a** (a) and **14b** (b) in $CDCl_3$. Shown are chemical shifts of the NH (2.96 ppm and 1.70 ppm in the case of **14a** and **14b**, respectively), CH_2 and OCH_3 / CH_3 signals of **14a** / **14b** ([**14a**] = [**14b**]).